

# Antenna Evaluation for Vehicular Applications in Multipath Environment

Edith Condo Neira



**CHALMERS**

Communication Systems Group  
Department of Signals and Systems  
Chalmers University of Technology

Gothenburg, Sweden 2017

Edith Condo Neira  
Antenna Evaluation for Vehicular Applications in Multipath Environment

Department of Signals and Systems  
Technical Report No R002/2017  
ISSN 1403-266X

Communication System Group  
Department of Signals and Systems  
Chalmers University of Technology  
SE-412 96 Göteborg, Sweden  
Telephone + 46 (0)70-574 5301  
Email: edith.condo.neira@chalmers.se

Copyright ©2017 Edith Condo Neira  
except where otherwise stated.  
All rights reserved.

Printed by Chalmers Reproservice,  
Gothenburg, Sweden, March 2017.

*To Felicia & Stefan*

*“La vida no se trata de como sobrevivir a una tempestad sino como  
bailar bajo la lluvia.”*

*– Unknown*



# Abstract

Antennas are essential components in any wireless communication system. To evaluate them is challenging, especially when new technologies are emerging.

Future intelligent transport systems, where vehicular communications play an important role will cover important aspects such as traffic safety and traffic efficiency. These applications will be covered by technologies such as IEEE 802.11p and LTE. For these emerging technologies, traditional methods for measuring the vehicular antennas such as anechoic chamber measurements or expensive and time-consuming field measurements may not be enough or suitable. Thus a new method for evaluating the antennas performance is desirable. A method that includes the multipath environment to give an idea of the antenna performance in the whole system and at the same time be able to be applied at early stages of product development. This thesis aims to provide such method.

The thesis is divided in two parts. The first part contains an overview and background of important concepts needed for development of methods for evaluation of vehicular antennas. In the second part, the papers that constitute the core of this work are appended.

In Paper A, we evaluate the vehicle's antenna performance using only simulations. We start by defining the multipath environment for vehicle-to-vehicle and vehicle-to-infrastructure (V2X) communication. Then, the V2X environment is simulated using a multipath simulation tool to evaluate the vehicle's antennas radiation patterns placed at different positions on the vehicle. This will result in the received power cumulative distribution functions (CDFs) for the voltage samples at the receiving antennas port.

In Paper B, we present the design and evaluation of an antenna module for IEEE 802.11p and LTE technologies. The module is designed taking into consideration the available space and suitable placement on the vehicle. The proposed module is in accordance with the requirements for LTE and IEEE 802.11p technologies. This is validated with the analysis of the antenna efficiencies, S-parameters, radiation patterns, and diversity performance for the simulated and measured antenna module.

Finally, Paper C presents a method for the evaluation of V2V antennas in a simulated measurement-based multipath environment. Here, a measurement campaign is performed to obtain the parameters (i.e., the angular received power spectrum) that define a realistic V2V multipath environment. These parameters are then introduced in a multipath simulation tool where the antennas radiation patterns are evaluated. Results are expressed in terms of received power CDFs. This method is validated by comparing the simulated and measured received power for two roof-top vehicle antennas.

**Keywords:** Vehicular antenna evaluation, V2V measurements, V2V simulations, multipath environment, IEEE 802.11p, LTE.

# List of Included Publications

The thesis is based on the following appended papers

- [A] E. Condo Neira, U. Carlberg, J. Carlsson, K. Karlsson, and E. G. Ström, "Evaluation of V2X Antenna Performance Using a Multipath Simulation Tool," *Antennas and Propagation (EuCAP) Proceedings of the 8th European Conference*, The Hague, The Netherlands, April 2014.
- [B] E. Condo Neira, J. Carlsson, K. Karlsson, and E. G. Ström, "Combined LTE and IEEE 802.11p Antenna for Vehicular Applications," *Antennas and Propagation (EuCAP) Proceedings of the 9th European Conference*, Lisbon, Portugal, April 2015.
- [C] E. Condo Neira, K. Karlsson, E. G. Ström, J. Carlsson, and A. Majidzadeh, "V2V Antenna Evaluation Method in a Simulated Measurement-Based Multipath Environment," submitted to *IEEE Transaction on Antennas and Propagation*, Dec. 2016.



# Acknowledgments

First and foremost, I would like to express my gratitude to my main supervisor Prof. Jan Carlsson at early stages and Prof. Erik Ström my examiner and main supervisor in the last stage of this work. Thanks for all the fruitful discussions, for your support and guidance. It has been a privilege to work under your supervision. I've learned a lot from you both.

I would also like to thank my co-supervisor and colleague Dr. Kristian Karlsson at SP Technical Research Institute of Sweden. Your enthusiasm, interesting discussions, availability and support are deeply appreciated. I should not forget to thank all my colleagues at SP. In particular, I would like to thank Peter Ankarson for helping me with software simulations. Niklas Arabäck and Olof Johansson should also be mentioned. Thanks for being there when times were tough.

Furthermore, I would like to thank to all the people at the Communication and Systems Group at Chalmers. It has been a pleasure to be part of this amazing group. Special thanks go to Agneta and Natasha for helping me with administrative matters and for always welcoming me every time I visited Chalmers. I also want to thank all the members of the CHASE V2X Antenna project for all the interesting discussions we had during the project. In particular, I'm grateful to Amir Majidzadeh at Volvo Cars for providing me with vehicles for testing.

For valuable discussions, good cooperation and friendship I want to thank Dr. Per Landin and Dr. Ulf Carlberg. Even though you both have a lot to do you always have the time to answer my questions. I am also grateful to all my friends, those who have helped me and supported me in various ways along this work.

I would also like to thank my family for their support, encouragement, and their unconditional love over the years. Dear mom and dad, I am forever indebted to you for giving me the opportunities and experiences that have made me who I am.

Last but not least, my warmest thanks to my lovely daughter and my beloved husband. You both mean the world to me. I am so lucky to have you by my side. My little heart Felicia, you are my source of inspiration, your smile light up my days and make me keep going. Dear Stefan thanks for your support, understanding, unfailing love, and for being with me in every decision I take. This work is dedicated to you both.

Edith Graciela Condo Neira

Gothenburg, March 2017

This work has been supported by SP Technical Research Institute of Sweden (SP) and partly supported by the Swedish Governmental Agency for Innovation Systems (VINNOVA) within the VINN Excellent Center CHASE.

# Acronyms

AoA:	Angle-of-arrival
CDF:	Cumulative distribution function
CSI:	Channel state information
DSRC:	Dedicated short-range communication
ETSI:	European telecommunication standards institute
GPS:	Global positioning system
GUI:	Graphical user interface
ITS:	Intelligent transport system
LOS:	Line-of-sight
LTE:	Long term evolution
MIMO:	Multiple-input multiple-output
NLOS:	Non-line-of-sight
PIFA:	Planar inverted F-antenna
RIMP:	Rich isotropic multipath
RLOS:	Random-line-of-sight
SDARS:	Satellite digital audio radio service
V2I:	Vehicle-to-infrastructure
V2V:	Vehicle-to-vehicle
V2X:	Vehicle-to-vehicle and vehicle-to-infrastructure



# Contents

<b>Abstract</b> .....	<b>i</b>
<b>List of Included Publications</b> .....	<b>iii</b>
<b>Acknowledgments</b> .....	<b>v</b>
<b>Acronyms</b> .....	<b>vii</b>
<b>I Overview</b> .....	<b>1</b>
<b>1 Introduction</b> .....	<b>1</b>
1.1 Objective.....	2
1.2 Thesis Outline.....	3
<b>2 Wireless Propagation</b> .....	<b>5</b>
2.1 Random Line-Of-Sight (RLOS).....	5
2.2 Rich Isotropic Multipath (RIMP).....	6
2.3 Weighted Environment for Vehicular Applications.....	6
2.4 Wireless Propagation Emulation .....	7
<b>3 Antenna Characteristics</b> .....	<b>11</b>
3.1 S-parameters .....	12
3.2 Total Radiation Efficiency and Radiation Efficiency.....	13
3.3 Radiation Pattern .....	13
3.4 Diversity .....	15
<b>4 Antennas for Vehicular Applications</b> .....	<b>17</b>
4.1 802.11p Antennas .....	17
4.2 LTE Antennas.....	18
4.3 Combined Antenna Module .....	19
<b>5 Novel Vehicular Antenna Evaluation Method</b> .....	<b>21</b>
5.1 Propagation Model .....	21
5.2 Measurement Campaign.....	22
5.3 Antenna Evaluation Method and a GUI.....	23
5.4 GUI example .....	25
<b>6 Conclusions and Future Work</b> .....	<b>27</b>
6.1 Contributions .....	27

6.2	Conclusions .....	28
6.3	Future work.....	28
	<b>References .....</b>	<b>30</b>
<b>II</b>	<b>Included Papers.....</b>	<b>33</b>

# **Part I**

## **Overview**



# Chapter 1

## 1 Introduction

Wireless communication involves the transmission of information over a distance without using cables, wires or any other forms of electrical conductors. It is the oldest form of communication and it has experienced an enormous growth in the last few decades. Everything started with smoke signals, drums, semaphore flags, etc. followed by the telegraph and later by the telephone [1]. This technology took off with the discovery of electromagnetic waves. Thanks to physicists and scientists, we have the basis that is needed for the continuous growth of this technology which has several applications, e.g., cellular, satellite or vehicular communications. Cellular communications is one of the applications that have experienced an exponential growth. It has evolved from analog systems (i.e., 1G) to 2G, 3G, 4G, and beyond. These applications would not be possible without the use of antennas since they are one of the key components of any wireless communication system, enabling transmission and reception of propagating signals.

In cellular communications the evaluation of the antennas is well explored. For this application, the antenna may be measured in an anechoic chamber to find the line-of-sight (LOS) properties or in a reverberation chamber when non-line-of-sight (NLOS) or multipath components are expected. The latter may be caused by multipath phenomena such as reflection, scattering and diffraction. Unlike cellular communications, in vehicular communications there are still a lot to be explored when it comes to the evaluation of antennas, especially nowadays when new technologies are emerging and are intended to be implemented (e.g., IEEE 802.11p, LTE, 5G).

The application of these new technologies will contribute to Intelligent Transport Systems (ITS). ITS have the potential to increase traffic safety, traffic efficiency and infotainment through the communication between vehicles and/or vehicles to infrastructure. Communication types such as Vehicle-to-Vehicle (V2V) and Vehicle-to-Infrastructure (V2I) together V2X communications are the basis for Cooperative-ITS (C-ITS). V2X can be supported by different technologies.

In Europe, V2V is standardized by European telecommunication standards institute (ETSI) as the ITS-G5 standard and in the United States is namely Dedicated Short-Range Communication (DSRC). Both ITS-G5 [2] and DSRC [3] are based on IEEE 802.11p and they operate in the 5.9 GHz band. For safety related applications, 802.11p is a suitable candidate due to low latency and communication range of several hundred meters [4]. In dense scenarios, where scalability problems may appear, a possible alternative for ITS may be Long Term Evolution (LTE) technology. The reliability of the application of

these technologies highly relies on the quality of the communication link, where antennas are one of the key components. Therefore finding an optimal antenna performance is important.

In vehicular communications, there are many factors that will be influencing the antenna performance, e.g., the placement of the antenna on the vehicle, the vehicle's large number of metallic objects, the frequency in which the antenna is operating together with the vehicle's shape, and the vehicle's mobility. These factors will have different impact depending on the technology that is used. Moreover the increasing number of antennas and the limited space on the vehicle due to aesthetic aspects requires the development and the use of multiband antennas integrated in a single module. These multiband antennas may be affected by effects such as mutual coupling or finite ground plane size. Considering the vehicles high mobility, the traditional methods for measuring the antennas may not be enough. Thus new methods need to be proposed.

For V2V communications, where the frequency is relatively high, i.e., 5.9 GHz, the radiation pattern of the antenna is more affected by the vehicle's shape than for other technologies operating at lower frequencies, e.g., LTE. Thus it is difficult to judge if the antenna performs well or not simply by looking at the radiation pattern. In addition, in V2V communications, the transmitting as well as the receiving antennas is placed on roughly the same height. Thus, scatters responsible for the multipath are located mostly in the horizontal plane. Therefore, the waves that are incident on the receiving antenna may come from arbitrary directions in azimuth but within a limited range of angles in elevation. Thus it is important to evaluate the antenna performance in realistic multipath environments as the incident waves' parameters such as Angle-of-Arrival (AoA), polarization, and power, depend on the multipath environment. A possible solution to this is to carry out field measurements [5]–[6]. However, they are expensive, time consuming and not even possible at early stages of product development. Then simulations become more attractive [7]–[8] since they are cost effective, less time consuming and they can be applied before any hardware is available. Then, when to use measurements or simulations? Is it good enough to rely on simulations?

## 1.1 Objective

The aim of this work is to provide a suitable and efficient method for evaluation of antenna performance under realistic conditions by using the radiation pattern of possible antenna designs in realistic multipath environments. The method involves measurements and simulations and is intended to be used at any stage of product development and should be able to help the antenna designer to evaluate the antenna parameters, antenna placement, antenna types or number of antennas with respect to the system performance.

## **1.2 Thesis Outline**

The structure of this thesis is organized as follows. Chapter 2 provides a brief introduction of wireless propagation environments as well as concepts such as Random Line-of-Sight (RLOS), Rich Isotropic Multipath (RIMP), weighted environment, and wireless propagation emulation are described. In Chapter 3, a brief overview of antenna theory used along this thesis as well as diversity concepts are given. Chapter 4 focuses on vehicular antennas for 802.11p and LTE technologies. In Chapter 5, a brief description of the proposed antenna evaluation method and a graphical user interface are presented. Finally, the contribution of this thesis as well as future work is summarized in Chapter 6.



# Chapter 2

## 2 Wireless Propagation

In a wireless communication system, the medium in which electromagnetic waves propagate from the transmitter to the receiver is called propagation channel, and the behavior in which electromagnetic waves propagate is called wireless propagation. In a wireless propagation environment the electromagnetic waves may take only the direct path which is known as LOS or may take several propagation paths (multipath). In LOS the wave incident to the receiving antenna is coming from only one direction. In real V2X situations, we usually don't have LOS conditions since there are many objects in the surroundings that cause multipath phenomena such as reflection, scattering and diffraction. In addition to that, the received signal is often obstructed in a multipath environment.

In this chapter, we discuss three different wireless propagation environments for antenna evaluation. In Section 2.1 and 2.2, we discuss two extreme environments that are relevant for mobile communications and a starting point for vehicular communications. In Section 2.3, we discuss an environment that is relevant for vehicular communication which is the main focus of this thesis. We then describe how a multipath environment can be emulated.

### 2.1 Random Line-Of-Sight (RLOS)

A Random Line-Of-Sight (RLOS) environment is an environment that is characterized by one incident wave on the receiving antenna, and this incident wave has an arbitrary incident direction and polarization. This is shown in Fig. 2.1, where the antenna pattern is placed at the origin of the coordinate system and that a line from the center of the red square to the origin defines the AoA of the incident wave. The polarization of the wave is indicated by the black line that is on the red square.

In wireless mobile communications, a moving user is communicating with a fixed base station. The base station is normally elevated and the mobile device has an arbitrary orientation. Therefore, from the mobile perspective, RLOS environment is one extreme environment relevant for evaluating the antenna performance [9].

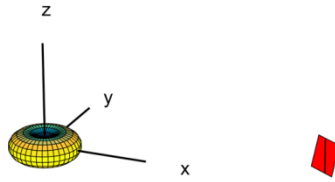


Figure 2.1. Visualization of a Random Line-Of-Sight (RLOS) environment in a specific time-instant.

## 2.2 Rich Isotropic Multipath (RIMP)

Unlike RLOS environment, RIMP environment is an environment which is characterized by many incident waves where the AoA of the waves are uniformly distributed over all directions in 3D space. In RIMP, the only antenna parameter that matters for a single antenna element is the total radiation efficiency. Fig. 2.2 shows the visualization of a RIMP environment where the waves are incident to the radiation pattern of an antenna that is placed at the origin of the coordinate system, e.g., a dipole antenna. As in Fig. 2.1, the incident waves are represented by the red squares and the polarization is indicated by the black lines on the red squares.

RIMP environment is another extreme environment to study the antenna performance for mobile communications [10], [11].

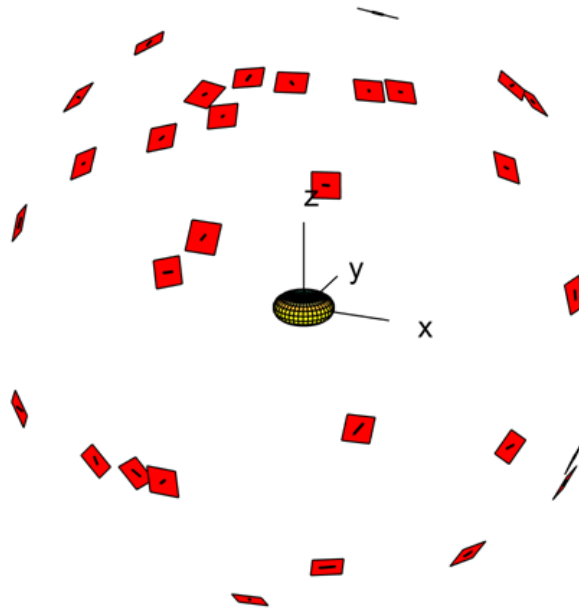


Figure 2.2. Visualization of a Rich Isotropic Multipath (RIMP) environment in a specific time-instant.

## 2.3 Weighted Environment for Vehicular Applications

As explained before, RLOS and RIMP environments are suitable environments for mobile communications but not for V2X applications since the vehicles are moving mostly in a horizontal plane and the antennas mounted on the vehicles are usually mounted at low heights. Then scatterers creating the multipath are located mostly in the horizontal plane. Thus, the environment for

vehicular applications is something in between RLOS and RIMP. Therefore, we define the environment for vehicular communications as a weighted environment [12] (Paper A).

In a weighted V2X environment, the waves that are incident on the receiving antenna will arrive from arbitrary directions in azimuth but within a limit range of angles in elevation. Each wave is vertically polarized. This assumption is described in [13] (Paper C).

In Fig. 2.3, the visualization of a weighted environment is given. This figure shows the incident waves in a specific time-instant which will be different in another time. In this example, we can see incident waves uniformly distributed in the whole horizontal plane with a limited angle of spread in elevation.

Unlike RIMP, the radiation pattern of the antenna is important in a weighted environment as it will be seen in the following chapter.

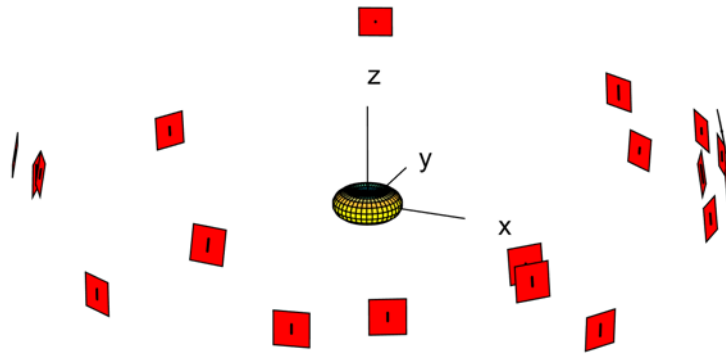


Figure 2.3. Visualization of a weighted environment in a specific time-instant.

## 2.4 Wireless Propagation Emulation

The discussed propagation environment may be emulated by anechoic chambers, reverberation chambers or by simulations. An anechoic chamber can be used to emulate a free space RLOS environment. This environment is a well-established reference environment for antennas mounted on roofs and masts with dominant LOS. However, modern antennas or terminals used for example in mobile communications cannot only be characterized in this environment since they need to be characterized in both extreme environments RLOS and RIMP [11].

RIMP can be emulated by reverberation chamber. Even though, anechoic chambers or reverberation chambers are very useful, there is still the need of simulation tools. Simulation tools are quite essential to try and test new ideas. They are repeatable, simple, fast and inexpensive.

In this thesis, we have used a wireless propagation simulation tool called ViRM-Lab (Visual Random Multi-path Environment Laboratory) [14]. ViRM-Lab is a computer code which generates a statistically fading environment by a number of statistically distributed incident waves. It uses antenna far-field

patterns and can simulate RLOS, RIMP and different kind of wireless propagation environments like a weighted environment.

In Fig. 2.4 and Fig. 2.5, the cumulative distribution functions (CDFs) as a function of the received power level are shown. Fig. 2.4 shows the comparison between RLOS and RIMP environments where three different antennas have been evaluated, i.e., a quarter-wave monopole centricly mounted on a  $1 \times 1 \text{ m}^2$  ground plane, a probe-fed patch with a ground plane size of  $20 \times 24 \text{ mm}$ , and a half-wave dipole antenna. The antennas have been evaluated in free-space and the far-field patterns are obtained from simulations performed in CST Microwave Studio [15]. Details of the antennas can be found in [12] (Paper A).

When computing the CDFs, we have used  $10^5$  realizations. Each realization contains one wave for RLOS and twenty waves for RIMP. The incident waves are distributed over the whole sphere and they present random polarization. It should be pointed out that the number of realizations should be large enough to determine the CDFs accurately and the number of incident waves for RIMP should be large enough to assure that the waves are distributed over the 3D sphere.

The CDFs results shown in Fig. 2.5 have been performed in a weighted propagation environment with vertically polarized incident waves that are uniformly distributed over the whole horizontal plane and with an angular spread in elevation between  $-5^\circ$  to  $15^\circ$ . The antennas that have been evaluated are a 5.9 GHz probe-fed patch antenna placed on the windscreen of a vehicle and a 5.9 GHz quarter-wave monopole antenna placed on the back of the vehicle's roof-top (shark-fin position). In this case, the monopole antenna performs better than the patch. This is because the monopole antenna presents an omnidirectional radiation pattern. As before, we have used  $10^5$  realizations and twenty incident waves.

As seen in Fig. 2.4 and Fig. 2.5, the directivity of the single port antenna is important in RLOS as well as in a weighted environment. In RIMP, the only antenna parameter that is important is the total radiation efficiency. The received power of RIMP will always follow the theoretical Rayleigh, see Fig. 2.4.

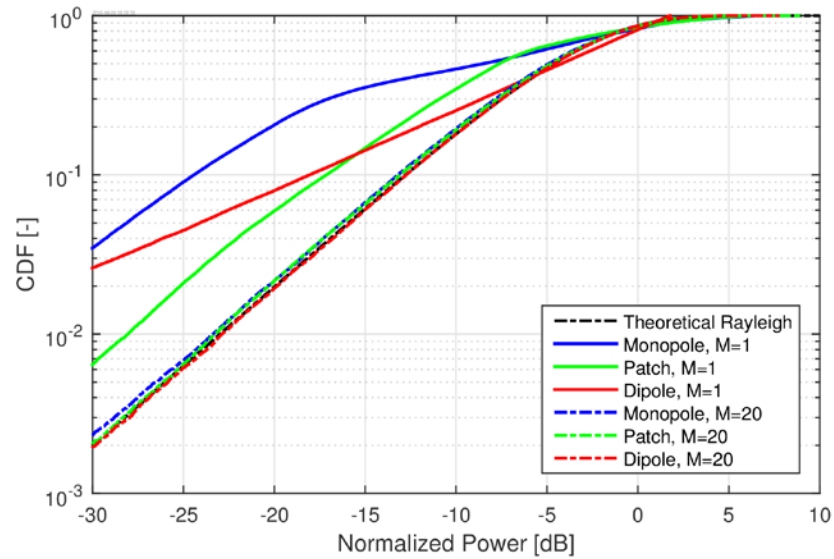


Figure 2.4. CDFs for linear polarized incident waves. Solid lines represent a RLOS environment ( $M=1$ ) and dashed lines represent a RIMP environment ( $M=20$ ).

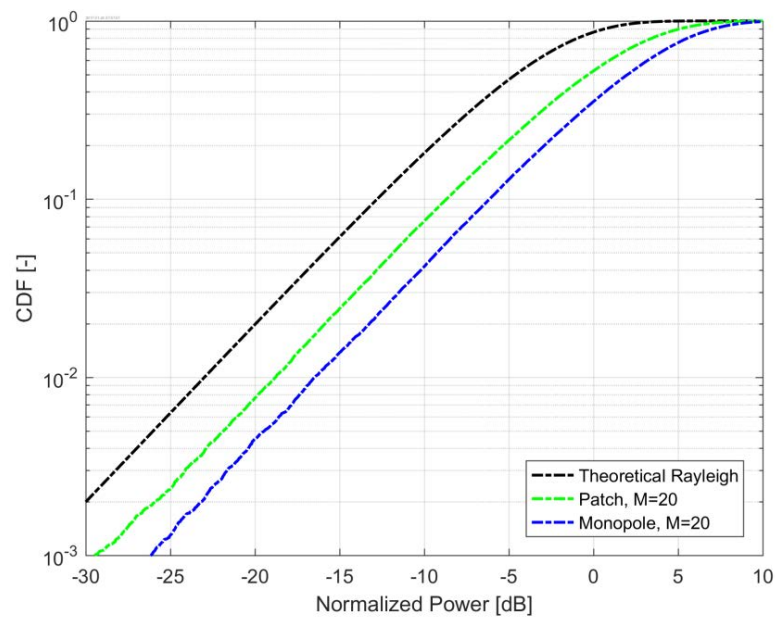


Figure 2.5. CDFs for vertically polarized incident waves in a weighted environment.



# Chapter 3

## 3 Antenna Characteristics

Antennas are one of the most important components in any wireless communications system since they are responsible to transmit or receive electromagnetic waves through a wireless propagation channel.

An antenna is usually designed to operate in one or several specific frequency bands. There are different types of antennas and the selection of any specific design depends on many factors, e.g., the type of application, available space, cost, etc., and most of the time compromises need to be done. The size of the antenna is often expressed in terms of the wavelength at the frequency of operation. The wavelength is given by

$$\lambda = \frac{c}{f} \quad (3.1)$$

where  $c = 3 \cdot 10^8$  m/s is the speed of light in free space and  $f$  is the frequency expressed in Hz.

Antennas can be classified in single-port antennas and multi-port antennas. Single-port antennas are antennas with one connector and they are the most common designs for automotive applications. Unlike single-port antennas, a multi-port antenna is an antenna with several radiating elements and several connectors. The main advantage of using multi-port antennas is that the signals from the several radiating elements can be combined in different ways, e.g., using diversity or multiple-input multiple-output (MIMO) schemes, and in this way the signal performance can be improved in comparison with a single-port antenna. An important parameter to be considered when designing a multi-port antenna is the distance between the antenna elements, which should be large enough in order to minimize mutual coupling. This can be quantified by measuring the antenna isolation (e.g., S21 in a two-port antenna).

Multi-port antennas are very useful in multipath environments since the waves that are incident to the antenna elements arrive from arbitrary directions, with arbitrary polarizations, phase and amplitudes. Application examples of multi-port antennas are in LTE and V2X communications. LTE requires the use of multi-port antennas in order to support MIMO schemes and V2X will benefit in using multi-port antennas since the complexity on the vehicle (i.e., the vehicle's shape) will have a great influence on the antenna radiation pattern.

In order to describe the characteristics of the antennas, definitions of various parameters are necessary. Therefore, in this chapter a brief overview of the antenna theory used in this thesis is given. In the first three sections of this

chapter, we describe the main antenna concepts and in the last section we briefly describe diversity.

### 3.1 S-parameters

Scattering parameters (S-parameters) describe the input-output relation between ports in an electrical system. The S-parameters can be calculated using network analysis techniques, more information can be found in [16]. Otherwise, they are often measured using a network analyzer.

Consider, a two-port network, shown in Fig. 3.1, where the incident voltage at port 1 and port 2 is denoted by  $V_1^+$ ,  $V_2^+$  respectively, and the leaving voltage, i.e., the reflected voltage is denoted by  $V_1^-$ ,  $V_2^-$ . The matrix elements  $S_{11}$ ,  $S_{12}$ ,  $S_{21}$ , and  $S_{22}$  are referred to as the S-parameters. The parameters  $S_{11}$ ,  $S_{22}$  are the reflection coefficient ( $\Gamma$ ) or return loss, and  $S_{12}$ ,  $S_{21}$  are the transmission coefficient from port 2 to port 1, and port 1 to port 2 respectively.

In a multi-port antenna, it is important to present an acceptable impedance match over the frequency band of operation. The antenna impedance match is most commonly characterized by the return loss represented by the S-parameter  $S_{11}$  which is typically measured in dB, see Fig. 3.2.  $S_{11}$  is defined as the ratio of the reflected wave to the incident wave. It is a measure of how much power supplied to the antenna reflects back. Ideally, all of the power supplied to the antenna is radiated with no reflections.

While measuring the impedance match is important, it is also important to measure the mutual coupling between the antennas since it degrades the antenna efficiency, and it can also alter the radiation pattern of the antennas. Mutual coupling can be quantified by measuring the antenna isolation which is represented by  $S_{21}$  in a two-port antenna.

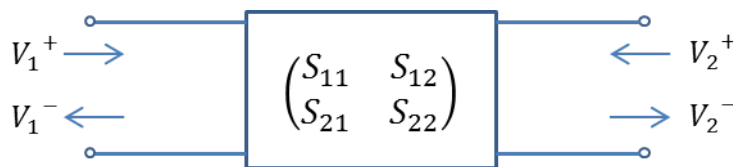


Figure 3.1. Transmitted and reflected waves in a two-port network.

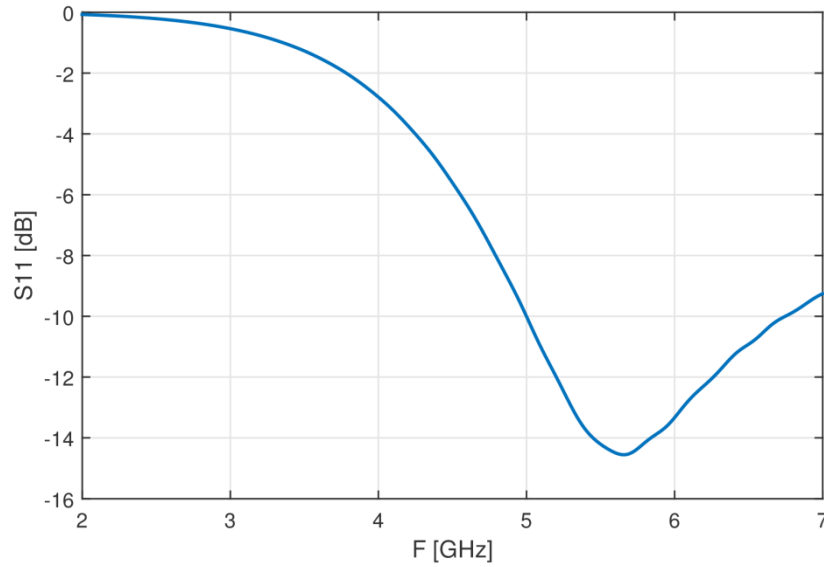


Figure 3.2. Reflection coefficient as a function of frequency for a monopole antenna designed for V2X communications. The antenna is mounted at the center of a finite size ground plane ( $1 \times 1 \text{ m}^2$ ).

### 3.2 Total Radiation Efficiency and Radiation Efficiency

The total radiation efficiency is the ratio between the radiated power and the incident power on the antenna port and is given by

$$\varepsilon_T = \varepsilon_R \cdot M \quad (3.2)$$

where  $\varepsilon_R$  is the radiation efficiency (i.e., the ratio between the radiated power to the input power of the antenna), and  $M$  is the mismatch factor caused by a reflection coefficient at the antenna port. The mismatch factor is given by

$$M = 1 - |\Gamma|^2 \quad (3.1)$$

The total radiation efficiency is the same as the radiation efficiency if there is no loss due to impedance mismatch. However, this is only possible in theory. In real life, some of the power incident to the antenna port is always lost. For example, power losses can be caused due to the mismatch between the antenna and the feeding network. Thus, the total radiation efficiency is always below 100 % (0 dB).

It should be pointed out that the equations above are applicable for single-port antennas. In multi-port antennas, the total embedded element efficiency at every port is the ratio between the radiated power and the input power at the port of interest while the other ports are terminated.

### 3.3 Radiation Pattern

Radiation pattern is a graphical representation of the radiation properties of an antenna as a function of space coordinates [17]. It may be represented in a 3D plot, or in 2D polar plots as shown in Fig. 3.3, and Fig. 3.4 respectively. Radiation patterns are usually normalized to the isotropic radiation level [18]. A pattern is isotropic if the radiation pattern is the same in all directions. In real

life, antennas with isotropic radiation pattern don't exist. However, they are used as comparison with real antennas.

In practice, all the antennas present a directional dependence. Even an omnidirectional antenna will present a directional dependence, even though its radiation pattern is characterized by an isotropic radiation in a single plane. The radiation pattern of the antennas is affected by the frequency of operation. The highest the frequency, the most variation should be expected. This can be seen in Fig. 3.3 and Fig. 3.4 which show a 3D plot and 2D plots, respectively of a quarter-wave monopole antenna. The antenna is placed on the roof-top of a vehicle and it resonates at 5.9 GHz.

In multi-port antennas when the radiation pattern is measured, the measured port is excited while the other ports are terminated by 50 ohm. This measurement can be done in an anechoic chamber. Otherwise, the radiation pattern may be obtained using full-wave simulations.

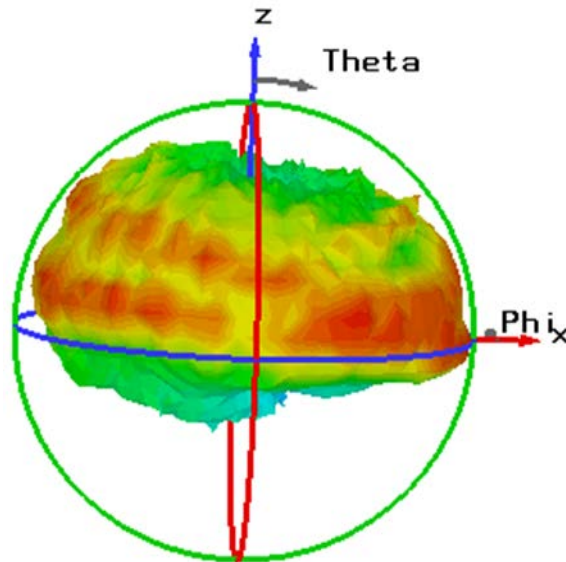


Figure 3.3. 3D radiation pattern of a quarter-wave monopole at 5.9 GHz. The antenna is mounted on the roof-top of a vehicle.

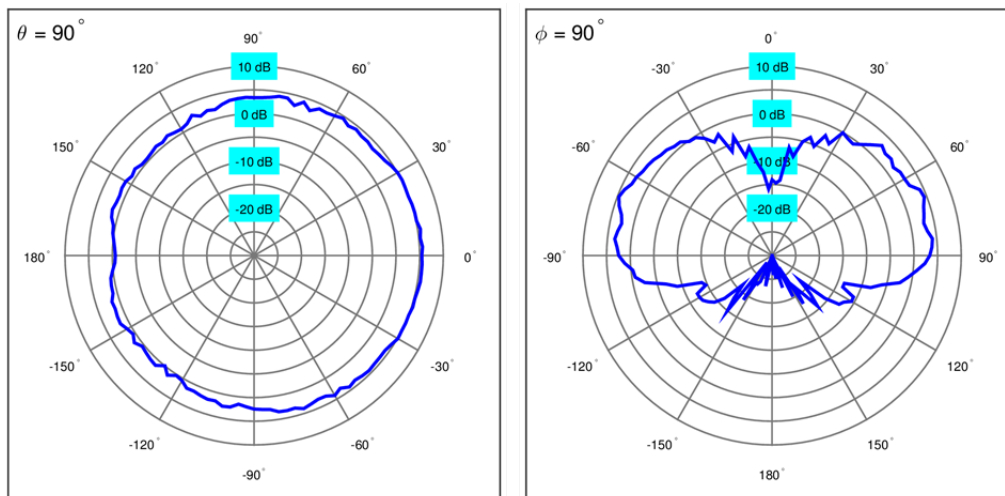


Figure 3.4. 2D polar radiation plot of a quarter-wave monopole at 5.9 GHz. The antenna is mounted on the roof-top of a vehicle. Left figure shows the radiation pattern in the horizontal plane and the right figure shows the elevation plane.

### 3.4 Diversity

Wireless communication systems may experience reflections from multiple scatterers, creating multipath channels, which are modeled as fading channels. If not properly designed, fading degrades the performance of a wireless system. One of the techniques to mitigate the effects of fading and improve system performance is MIMO.

MIMO is a technology that uses multiple antennas and it can be used to improve performance through diversity or to increase data rates through multiplexing [1]. Multiplexing consists in having multiple antennas at the transmitter as well as at the receiver. Thus the multiplexing gain is obtained from the fact that the MIMO channel can be separated into a number of parallel channels, more information can be found in [1]. Unlike multiplexing, diversity is also possible with a single antenna element at both ends. This is the case for time diversity and frequency diversity. For antenna diversity, which is another type of diversity technique, requires multiple antennas at the transmitter and/or at the receiver.

The idea of diversity is to send or receive the same information over independent fading channels. Reception over independent fading channels can be realized by spatial antenna diversity which is one of the most used diversity techniques [19]. For example, consider a case with two antennas at the receiving side. If the antennas are located far enough from each other (space diversity), it is unlikely that both antennas experience fading dips at the same time. Therefore, it is important to combine the signals properly. There are different diversity schemes to do this. In this thesis, we have used the selection combining scheme. Here, the receiver always selects the antenna with the strongest signal, detailed information about this and different diversity schemes can be found in [1].

Diversity performance is measured by diversity gain, and it is usually expressed in dB. Here, we won't go into details about different types of diversity gain, rather we refer to [18].

Fig. 3.5 shows how much a signal can be improved by applying diversity selection combining when two antennas are used. The antennas are designed for LTE communications to operate at three different frequency bands [20]. They are spatially separated by approximately  $\lambda/2$  at 2590 MHz. From the figure, it can be seen that the signal is improved by 5 dB when four or more incident waves are applied on the radiation patterns of the multi-port antennas.

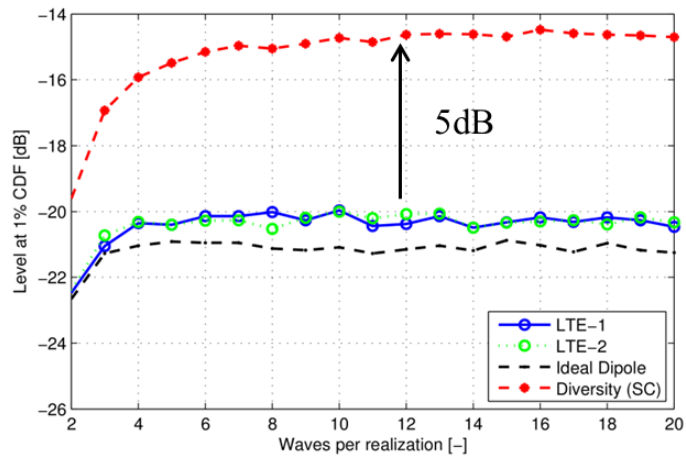


Figure 3.5. Received power level at 1% CDF level as a function of linearly polarized incident plane waves. The graph shows the diversity combined results when using a multi-port antenna for LTE.

# Chapter 4

## 4 Antennas for Vehicular Applications

Modern vehicles may contain multiple antennas for different wireless applications such as AM/FM radio, remote keyless entry, satellite navigation, satellite digital audio radio services, electronic toll collection, and others. All these applications are allocated at different frequency bands, covering frequencies from 0.5 MHz (AM radio) up to 77 GHz (Radar Collision System) [21]. In addition to the existing applications, modern vehicles are proposed to include IEEE 802.11p and LTE technologies. Both of them can contribute to ITS communications [4]. ITS communications aim to provide traffic safety, traffic efficiency and infotainment. For V2V communications, the leading technology is IEEE 802.11p due to its low latency, while LTE is currently restricted to V2X communications that is relatively latency-tolerant.

Even though vehicles are many wavelengths bigger than mobile phones at high frequencies, there are very limited available space and locations for placing an antenna. This is due to the design and aesthetic of the vehicles is very important. Therefore, traditional antennas are out of the scope when it comes to design. Thus, antenna engineers have to come up with new solutions like the development of multiband and multiport antennas integrated in a single module.

Aspects that should be considered when designing an antenna are the frequency of operation as well as the available location for placing the antenna on the vehicle. These two factors will affect the performance of the antenna considerably.

This chapter focuses on 802.11p and LTE technologies as well as the design and implementation of a combined antenna module including V2V and LTE antennas.

### 4.1 802.11p Antennas

For V2X communication, a suitable antenna candidate may be an omnidirectional antenna which radiates electromagnetic waves uniformly in all directions in the horizontal plane with the radiated power decreasing in elevation. This is taking into account that vehicles move mostly in the horizontal plane. Thus, communication between them occurs mostly in the horizontal plane. In the case of communication between vehicles and road infrastructure a certain degree in elevation should be considered.

Other types of antennas that may be considered are rectangular patch antennas, which are low profile antennas. These antennas are usually constructed on a dielectric surface. They may be a possible solution for V2X communications since they are cheap to manufacture and their gain is higher than an omnidirectional antenna. However, these antennas are directive and they radiate in a specific direction [17], [18]. Thus, they do not cover the whole horizontal plane. A solution to this could be placing the antennas at different positions on the vehicle, e.g., on the windscreen and rear window of the vehicle, as was done in [12] (Paper A). In this way, the horizontal plane can be covered.

Most of the measurement campaigns that have been carried out for V2X communications have used omnidirectional antennas [5], [6], [22-24]. The authors of [6] and [22] have used a short-circuited circular patch antenna. Antennas elements of this kind present omnidirectional pattern, for more information refer to [25]. The antenna was designed for a roof-top mounting position.

In this thesis, we have design a quarter-wave monopole antenna centrally mounted on a ground plane with size  $30 \times 30 \text{ mm}^2$ , and a probe-fed patch antenna, both of them resonating at 5.9 GHz and they are vertically polarized. The patch antenna has a length of 11 mm, width of 15 mm and a ground plane size of  $20 \times 24 \text{ mm}$ . The substrate is FR4 with a thickness of 1.6 mm, see Fig. 4.1.

These antennas have been mounted at different positions on the vehicle and they have been evaluated in different road traffic environments. The evaluation, placement and comparison between the antennas are explained in [12] (Paper A).

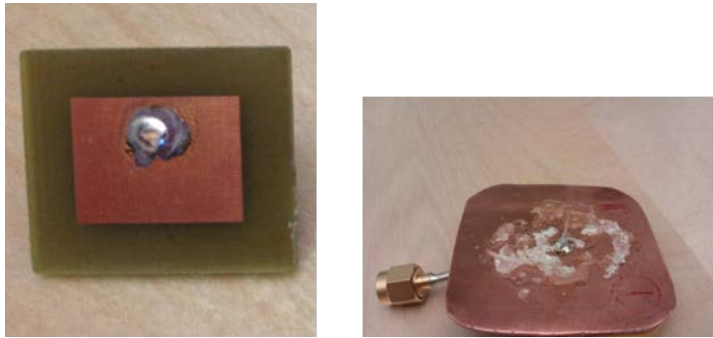


Figure 4.1. Antennas for V2X communication. Probe-fed patch antenna (left) and a quarter-wave monopole antenna (right).

## 4.2 LTE Antennas

In recent years, there is a considerable interest into LTE technology by the automotive industry. This is due to LTE is a possible alternative for ITS communications [4]. LTE presents high data rates for applications such as internet connectivity.

A considerable number of LTE antenna designs have been published in the literature. Most of them are for laptops [26], or for mobile devices [27-29]. These antennas are required to perform well at many frequency bands and to support multi-antenna techniques such as MIMO.

For vehicular applications, a few designs have been published [30], [31], [32]. These antennas are based on a monopole concept. In [30], they present a design which is intended to be mounted on the roof of large vehicles for public transportation. The authors of [31] and [32] present a roof-top LTE antenna design. The antenna is designed to be integrated in the shark-fin module on the roof-top on a vehicle.

Unlike previous research, our LTE antenna design is intended to be integrated into the rear-spoiler on a vehicle. The antenna prototype is based on a Planar Inverted F-Antenna (PIFA) [33]. The antenna has an omnidirectional behavior. It is vertically polarized, and it's designed to cover three frequency bands, see Table I.

**Table I. Frequency Bands for LTE**

LTE Frequency Bands	
<i>Uplink</i>	<i>Downlink</i>
698 - 716 MHz	925 - 960 MHz
1710 - 1785 MHz	2110 - 2170 MHz
2500 - 2570 MHz	2620 - 2690 MHz

For the design, we have focused on achieving the highest antenna matching, lowest mutual coupling and an omnidirectional radiation pattern performance. The antenna is shown in Fig. 4.2. The design parameters and results are presented in [20].

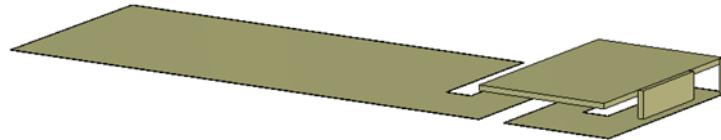


Figure 4.2. PIFA antenna for LTE communications.

### 4.3 Combined Antenna Module

As mentioned before, it is important to develop multiband antennas integrated in a single module to maintain the aesthetic of the vehicle. For example [34] has designed an antenna that covers both terrestrial services and satellite services. While [6], presents an antenna module including V2V, Global Positioning System (GPS) and LTE antennas. This module is placed on the roof-top on a vehicle.

In [20] (Paper B), we present an antenna module suitable to be integrated inside the rear-spoiler on a vehicle. The module consists of two identical LTE antennas and two identical V2X antennas. As mentioned before, the LTE antennas are based on a PIFA design. These antennas are printed on FR4 substrate with permittivity of 4.3, loss tangent of 0.025 and thickness of 1.6

mm. The antennas have individual ground planes, which are spatially separated by 50 mm, see Fig. 4.3. For V2X, we have used quarter-wave length monopole antennas. The antennas are placed on the ground plane of each LTE antenna as shown in Fig. 4.3 and they are spatially separated by 90 mm. The separation between the antennas is to achieve a good isolation as well as to have enough available space for future GPS, Satellite Digital Audio Radio Service (SDARS) antenna integration.

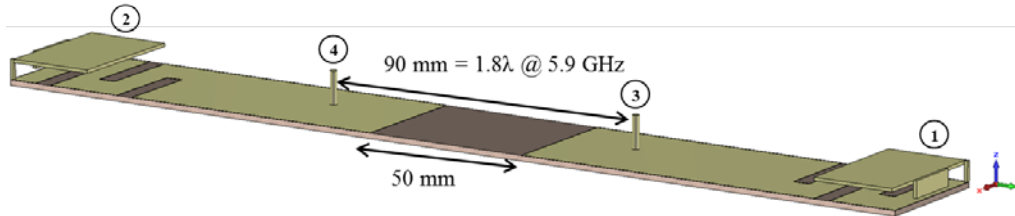


Figure 4.3. Antenna module for LTE and V2X communications.

The manufactured antenna module prototype is shown in Fig. 4.4. The dimensions of the module are 290 x 40 x 7.6 mm<sup>3</sup>. These dimensions are within the specification requirements which are given by the available space inside the rear-spoiler on a vehicle, e.g., crossover vehicle. Simulations and measurement results can be found in [20] (Paper B).



Figure 4.4. Manufactured prototype of the antenna module

# Chapter 5

## 5 Novel Vehicular Antenna Evaluation Method

The increasing number of antennas in the vehicles due to the desire of implementing new wireless technologies especially for making a more safe and efficient vehicle requires accurate and efficient methods for evaluating the antenna performance. These antennas must be evaluated in different multipath environments. A possible solution to this is to carry out measurement campaigns. However, they are expensive and time consuming. Therefore, simulations are more attractive. They are less time consuming, repeatable and they can be applied at any stage of product development.

In this chapter a general overview of the antenna evaluation method presented in [13] (Paper C) is discussed in Section 5.1 and Section 5.2. In Section 5.3 a graphical user interface is presented together with a brief description.

### 5.1 Propagation Model

A multipath environment can be simulated by using ray tracing approach as in [7]–[8], but could also be simulated by performing measurement campaigns since they can provide the information that is needed to emulate a multipath environment.

From a measurement campaign, we can obtain the angular power spectrum which can be used to simulate a multipath environment. We start by writing a general equation for the average received power at the antenna port due to an incident plane wave

$$\overline{P}_a = E \left[ |\mathbf{G}(\theta, \varphi) \cdot \mathbf{E}(\theta, \varphi)|^2 \right], \quad (5.1)$$

where  $E$  is the expectation operator,  $\mathbf{G}(\theta, \varphi)$  is the radiation field,  $\mathbf{E}(\theta, \varphi)$  is the incident complex electrical field,  $\theta$  is the polar angle, and  $\varphi$  is the azimuth angle of the incident field. Then some assumptions are made

- 1) The incident field consist of a number of vertically polarized, plane waves with statistically independent zero-mean complex Gaussian amplitudes.
- 2) The incident plane waves arrive in the horizontal plane and their angle of arrivals are uniformly distributed.
- 3) The angular power spectrum is constant in each of the four equal-sized sectors around the vehicle.

After the two first assumptions, we can express the average received power at the antenna port as

$$\overline{P}_a = E \left[ \left| \sum_{m=1}^M E_m^{(i)} W(\varphi_m) G(\varphi_m) \right|^2 \right] \quad (5.2)$$

Finally, considering the last assumption, the above equation is simplified as

$$\overline{P}_a = \sigma^2 \left( W_F^2 |G_F|^2 + W_L^2 |G_L|^2 + W_B^2 |G_B|^2 + W_R^2 |G_R|^2 \right), \quad (5.3)$$

where  $W_x^2$  is piece-wise constant in the forward, left, back and right sectors, and  $|G_x|^2$  is proportional to the average power gain in the sector  $X \in \{F, L, B, R\}$ . The full derivation of these equations can be found in the attached Paper C.

## 5.2 Measurement Campaign

In order to estimate the parameters that describe the multipath environment a measurement campaign was performed.

Fig 5.1 shows a block diagram of the steps to follow to obtain the parameters that were needed to simulate a multipath environment.

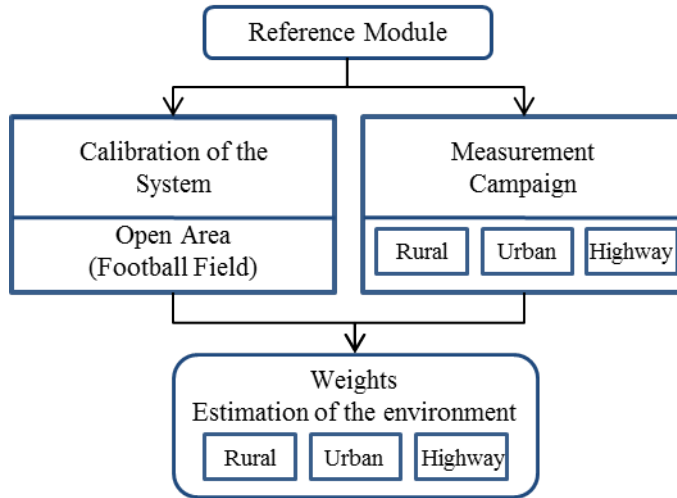


Figure 5.1. Block diagram to obtain the weights.

We started by designing a reference module which consists in four identical 5.9 GHz probe-fed patch antennas oriented outwards and placed far from each other, see Fig. 5.2.



Figure 5.2. Reference module mounted on the vehicle. The red circles show the placement of the antennas.

The reference module was used for the calibration of the system and for the measurement campaign. The calibration of the system was performed in an open area to obtain the reference antenna gain, and the measurement campaign was performed to obtain the average received power in three different road traffic environments (rural, urban, and highway). In both cases, two vehicles were used. On the transmitter side a 5.9 GHz quarter-wave monopole antenna was used. The antenna was mounted on the roof-top of the vehicle, and on the receiver side the reference module was used, see Fig. 5.2.

Once the reference antenna gain as well as the average received power for the four antennas used in the reference module are obtained, then the parameters that describe the multipath environment ( $W_L$ ,  $W_B$ ,  $W_R$ ) can be calculated. This is done by solving (5.3), where  $W_F$  is normalized to 0 dB.

### 5.3 Antenna Evaluation Method and a GUI

For the evaluation of the described method a graphical user interface (GUI) has been designed as shown in Fig. 5.3.

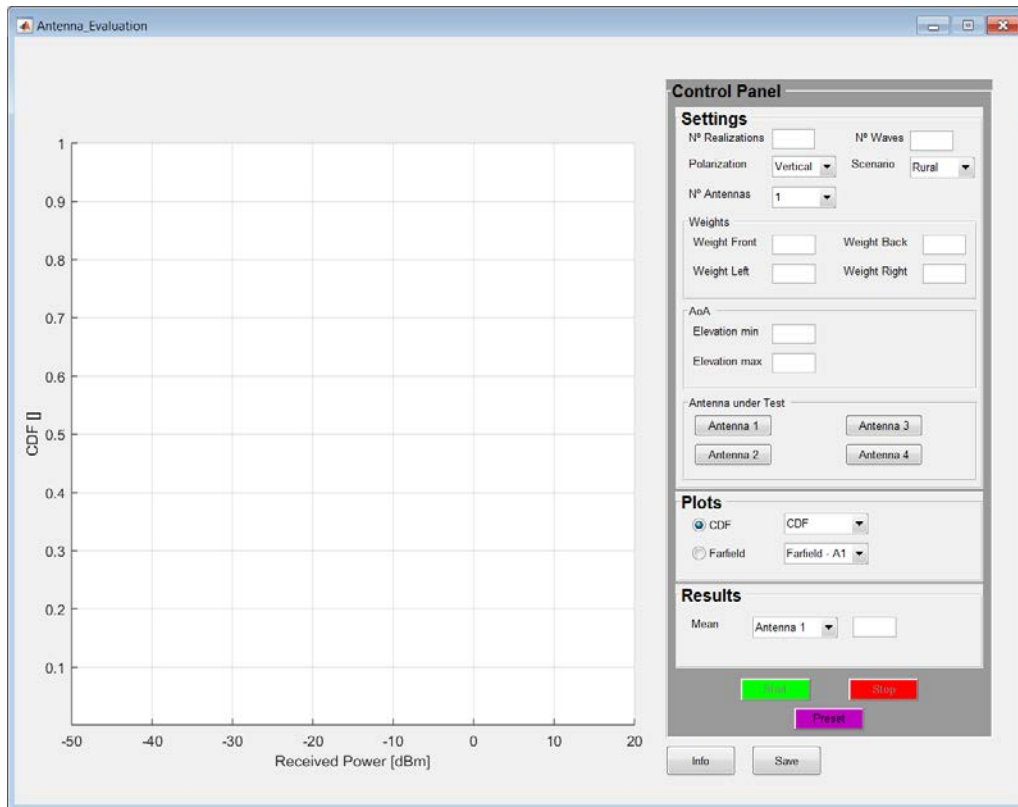


Figure 5.3. GUI for the evaluation of the antennas.

The GUI consists in a control panel divided in settings which are defined by the user, plots which show the graphical results according to the settings, and results which show a numerical value obtained from the plots.

### 5.3.1 Settings

The user defines the settings as follow

- **N° Realizations:** In order to simulate a changing environment as it is in reality a large number of realizations should be chosen. An appropriate number could be  $10^4$  or  $10^5$ . The larger the number of realization the better accuracy for low CDF values. However, the simulation time is longer.
- **N° Waves:** The number of incident waves should be chosen to assure that each sector get at least one incident wave. An appropriate number is twenty waves.
- **Polarization:** The user can choose between vertical, horizontal, and random (i.e., vertical, and horizontal) polarization.
- **Scenario:** The user can choose between rural, urban, and highway environment where each environment has its own weights.
- **Number of Antennas:** The user can choose between one to four antennas. The number of antennas chosen here are the number that should be uploaded in antennas under test.

- **Weights:** The weights are the parameters calculated in [13] (Paper C). These are set automatically when the scenario is selected. User defined weights can be entered manually.
- **Angle-of-Arrival (AoA):** The minimum and maximum AoA of the incident plane waves with respect to the elevation angle ( $\theta$ ) should be written here. The range of the elevation minimum value is between  $0^\circ$  to  $90^\circ$  and for the elevation maximum value the range is between  $90^\circ$  to  $180^\circ$ .
- **Antenna under Test:** The far-field pattern imported as ASCII.txt file from CST should be uploaded here.

### 5.3.2 Plots

- **CDF:** The user can choose between CDF, CDF and theoretical Rayleigh, and 1% CDF level.
- **Farfield:** The user can choose between Farfield and Farfield & Waves.

### 5.3.3 Results

- **Mean:** It shows the average received power of the antennas under test.

## 5.4 GUI example

Fig. 5.4 shows an example of the GUI where two probe-fed patch antennas have been evaluated. The antennas have been designed to operate at 5.9 GHz and they are placed on the roof-top of the vehicle as shown in Fig. 5.5.

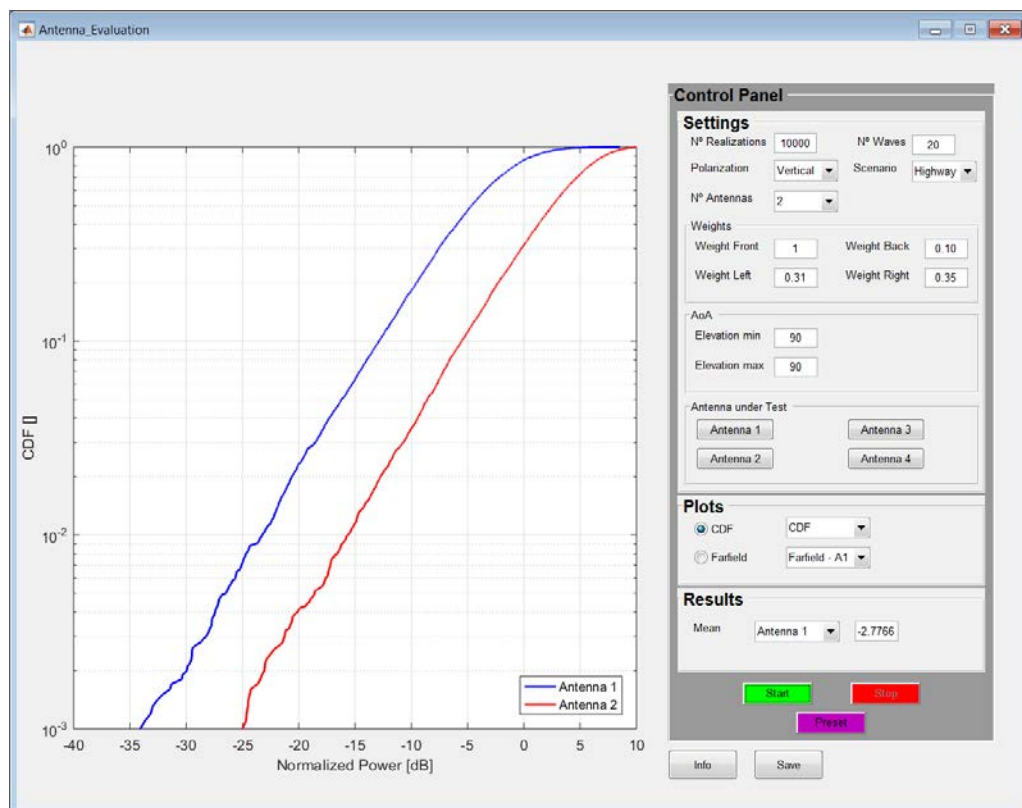


Figure 5.4. An example using the GUI.

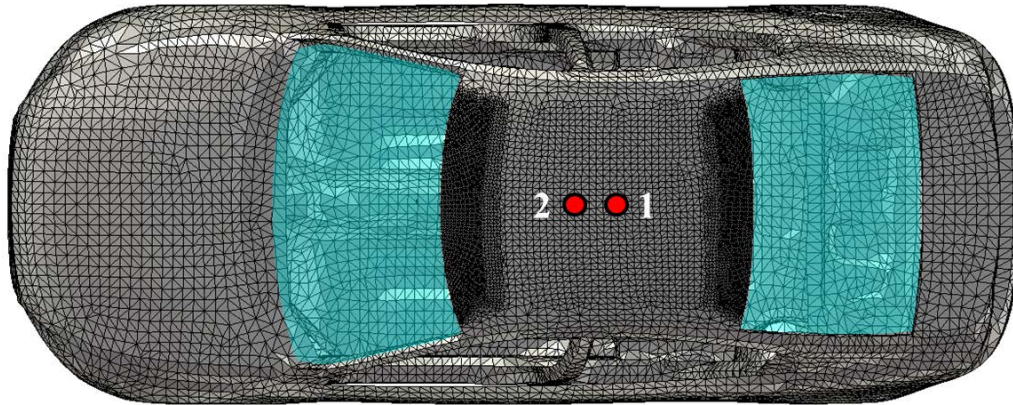


Figure 5.5. Placement of the antennas that are used in a GUI.

# Chapter 6

## 6 Conclusions and Future Work

This chapter summarizes the main contributions of this thesis to the research field. In Section 6.1, we summarize each of the three appended papers. In Section 6.2, conclusions are given and in the last section some ideas on future work are presented.

### 6.1 Contributions

#### 6.1.1 Paper A: Evaluation of V2X Antenna Performance Using a Multipath Simulation Tool

In this paper, we present a method for evaluating the V2X antennas performance. The method is based on simulations. First we start by defining a multipath environment for V2X communications, i.e., weighted environment. In a weighted environment, the waves that are incident on the receiving antenna will come from arbitrary directions in azimuth, but within a certain range of angles in elevation. Then, this environment is simulated in a multipath simulation tool and applied to the antennas radiation patterns and the evaluated results are presented in terms of the received power CDFs.

This simulated method has been applied to two different V2X antennas placed at different positions on the vehicle. Results show that the method is efficient, fast, and it can be applied to evaluate different antenna types, and positions. The importance of having antennas with radiation patterns covering the whole azimuth plane is also emphasized.

#### 6.1.2 Paper B: Combined LTE and IEEE 802.11p Antenna for Vehicular Applications

Nowadays, the increasing number of antennas and the restricted space due to aesthetic aspects on the vehicle emphasizes the importance to have multiband antennas integrated in a single module. In this paper, we design a compact antenna module for LTE and IEEE 802.11p technologies that could be easily integrated inside the rear spoiler on a vehicle. The module consists of two identical quarter-wave monopoles for V2X applications and two identical printed inverted F-antennas for LTE communications. In both cases the antennas radiation patterns cover the whole azimuth plane. The module has been evaluated by analyzing the antenna efficiencies, S-parameters, radiation patterns, and by calculating diversity performance. Results of our proposed module are in accordance with LTE and IEEE 802.11p requirements.

### **6.1.3 Paper C: V2V Antenna Evaluation Method in a Simulated Measurement-Based Multipath Environment**

In this paper, a method for evaluating V2V antenna performance under realistic conditions is presented. As was done in Paper A, first we start by defining the V2V environment. Then, we use the antenna radiation pattern (obtained from full-wave simulation software) in combination with a multipath simulation tool which generates a realistic multipath environment. In order to obtain the parameters that define the realistic multipath environment a measurement campaign was performed in three different road traffic environments. Then, these parameters are used in the multipath simulation tool to generate a realistic multipath environment. The accuracy of the method is validated by comparing the simulated and measured received power for two roof-top vehicle antennas.

Results show that the method is fast and efficient and it can be applied at early stages of product development.

## **6.2 Conclusions**

Through this thesis we have developed a method for evaluating the vehicular antenna performance for ITS applications with emphasis on V2V communications. We have seen that in order to evaluate the antenna performance it is important to consider the multipath environment. This environment may be simulated as in Paper A, and Paper B or may be estimated based on field measurements as in Paper C.

Then, when to use simulations or measurements? Simulations are usually fast in comparison with measurements. They are repeatable and can be applied at early stages of product development. However, to give a meaningful evaluation of the antenna performance for ITS vehicular applications it is important to consider a realistic multipath environment. Such environments can only be obtained by performing field measurements, as has been done in Paper C. Therefore, instead of using only simulations, we propose a method that uses simulations to evaluate the antenna performance in a measurement-based multipath environment. Results, presented in a GUI, show that the method is fast, accurate, and it can be applied as an alternative to field measurements. Moreover, the method can be used at early stages of product development, and it can become a helpful tool for antenna designers.

## **6.3 Future work**

The increasing number of antennas on vehicles due to the development of new technologies requires methods that are repeatable, fast and accurate. These methods should include the multipath environment.

A further extension of this work may be to generate a multipath environment for LTE communications, or 5G, and apply our proposed method.

---

Another interesting area may be to study another traffic scenario than a convoy scenario.

## References

- [1] A. Goldsmith, *Wireless Communications*, First ed. New York, USA: Cambridge University Press, 2005.
- [2] E. G. Ström, "On Medium Access and Physical Layer Standards for Cooperative Intelligent Transport Systems in Europe," *Proceedings of the IEEE*, vol. 99, no. 7, pp. 1183-1188, July 2011.
- [3] J. B. Kenney, "Dedicated Short-Range Communications (DSRC) Standards in the United States," *Proceedings of the IEEE*, vol. 99, no. 7, pp. 1162-1182, July 2011.
- [4] J. Calabuig, J. F. Monserrat, D. Gozálviz, and O. Klemp, "Safety on the Roads LTE Alternatives for Sending ITS Messages," *IEEE Vehicular Technology Magazine*, pp. 61-70, Jan. 2015.
- [5] T. Abbas, J. Karedal, and F. Tufvesson, "Measurement-Based Analysis: The Effect of Complementary Antennas and Diversity on Vehicle-to-Vehicle Communication," *IEEE Antennas and Wireless Propagation Letters*, vol. 12, pp. 309-312, Mar. 2013.
- [6] M. Gallo, S. Bruni, M. Pannozzo, and D. Zamberlan, "Performance Evaluation of C2C antennas on Car Body," presented at the *Antennas and Propagation (EuCAP) 7th European Conference*, Gothenburg, Sweden, April 2013.
- [7] L. Reichardt, J. Pontes, W. Wiesbeck, and T. Zwick, "Virtual Drives in Vehicular Communication Optimization of MIMO Antenna Systems," *IEEE Vehicular Technology Magazine*, pp. 54-62, June 2011.
- [8] D. Kornek, M. Schack, E. Slotke, O. Klemp, I. Rolfes, and T. Kürner, "Effects of Antenna Characteristics and Placements on a Vehicle-to-Vehicle Channel Scenario," presented at the *IEEE International Conference on Communications Workshops (ICC)*, Capetown, South Africa, May 2010.
- [9] P. S. Kildal, U. Carlberg, and J. Carlsson, "Definition of Antenna Diversity Gain in User-Distributed 3D-Random Line-of-Sight," *Journal of Electromagnetic Engineering and Science*, vol. 13, pp. 86-92, June 2013.
- [10] P. S. Kildal and J. Carlsson, "New Approach to OTA Testing: RIMP and pure-LOS as Extreme Environments & a Hypothesis," presented at the *Antennas and Propagation (EuCAP) 7th European Conference*, Gothenburg, Sweden, April 2015.
- [11] J. Carlsson, U. Carlberg, and P. S. Kildal, "Diversity Gains in Random Line-Of-Sight and Rich Isotropic Multipath Environment," presented at the *Loughborough Antennas & Propagation Conference (LAPC)*, Loughborough, UK, Nov. 2012.
- [12] E. Condo Neira, U. Carlberg, J. Carlsson, K. Karlsson, and E. G. Ström, "Evaluation of V2X Antenna Performance Using a Multipath Simulation Tool," presented at the *Antennas and Propagation (EuCAP) 8th European Conference*, The Hague, The Netherlands, April 2014.
- [13] E. Condo Neira, K. Karlsson, E. G. Ström, J. Carlsson, and A. Majidzadeh, "V2V Antenna Evaluation Method in a Simulated Measurement-Based Multipath Environment," *submitted to IEEE Transaction on Antennas and Propagation*, Dec. 2016.

- [14] U. Carlberg, J. Carlsson, A. Hussain, and P. S. Kildal, "Ray Based Multipath Simulation Tool for Studying Convergence and Estimating Ergodic Capacity and Diversity Gain for Antennas with Given Far-Field Functions," presented at the *in 20th Internat. Conf. on Applied Electromagnetics and Communications (ICECom)*, Dubrovnik, Croatia, Sept. 2010.
- [15] *CST Microwave Studio*. Available: <https://www.cst.com/>
- [16] D. M. Pozar, *Microwave Engineering*, Third ed.: John Wiley & Sons, 2005.
- [17] C. A. Balanis, *Antenna Theory Analysis and Design*, Third ed. New Jersey, U.S.: John Wiley & Sons, 2005.
- [18] P. S. Kildal, *Foundations of Antenna Engineering A Unified Approach for Line-Of-Sight And Multipath*: Kildal, 2015.
- [19] A. F. Molisch, *Wireless Communication*: John Wiley & Sons Ltd, England, 2006.
- [20] E. Condo Neira, J. Carlsson, K. Karlsson, and E. G. Ström, "Combined LTE and IEEE 802.11p Antenna for Vehicular Applications," presented at the *Antennas and Propagation (EuCAP) 9th European Conference*, Lisbon, Portugal, April 2015.
- [21] V. Rabinovich, N. Alexandrov, and B. Alkhateeb, *Automotive Antenna Design and Applications*. New York, U.S.: Taylor and Francis Group, LLC, 2010.
- [22] O. Klemp, "Performance Considerations for Automotive Antenna Equipment in Vehicle-to-Vehicle Communications," *URSI International Symposium on Electromagnetic Theory*, pp. 934-937, Aug. 2010.
- [23] L. Reichardt, T. Fügen, and T. Zwick, "Influence of Antennas Placement on Car to Car Communications Channel," presented at the *Antennas and Propagation (EuCAP) 3rd European Conference*, Berlin, Germany, Mar. 2009.
- [24] S. Kaul, K. Ramachandran, P. Shankar, S. Oh, M. Gruteser, I. Seskar, *et al.*, "Effect of Antenna Placement and Diversity on Vehicular Network Communications," *Sensor, Mesh and Ad Hoc Communications and Networks (SECON)* pp. 112-121, June 2007.
- [25] V. Gonzales-Posadas, D. Segovia-Vargas, E. Rajo-Iglesias, J.L. Vazquez-Roy, and C. Martin-Pascual, "Approximate Analysis of Short Circuited Ring Patch Antenna Working at TM<sub>01</sub> Mode," *IEEE Transactions on Antennas and Propagation*, pp. 1875 - 1879, June 2006.
- [26] J. Lu and F. Tsai, "Planar Internal LTE/WWAN Monopole Antenna for Tablet Computer Application," *IEEE Transactions on Antennas and Propagation*, vol. 61, pp. 4358-4363, Aug. 2013.
- [27] I. Dioum, A. Diallo, S. M. Farssi, and C. Luxey, "A Novel Compact Dual-Band LTE Antenna-System for MIMO Operation," *IEEE Transactions on Antennas and Propagation*, vol. 62, pp. 2291-2296, April 2014.
- [28] O. A. Saraereh, C. J. Panagamuwa, and J. C. Vardaxoglou, "Wideband Slot Antenna for Low-Profile Hand-held Phone Applications Using Novel Decoupling Slots in Ground Plane," presented at the

- Loughborough Antennas & Propagations Conference (LAPC)*, Loughborough, UK, Nov. 2013.
- [29] Y. Hong, J. Lee, and J. Choi, "Design of a Multi-Band Antenna for 4G Wireless Systems," presented at the *Antennas and Propagation (EuCAP) 8th European Conference*, The Hague, The Netherlands, April 2014.
- [30] B. Sanz-Izquierdo and R. Leelaratne, "Evaluation of Wideband LTE Antenna Configurations for Vehicular Applications," presented at the *Loughborough Antennas & Propagations Conference (LAPC)*, Loughborough, UK, Nov. 2013.
- [31] A. Thiel, L. Ekiz, O. Klemp, and M. Schutz, "Automotive Grade MIMO Antenna Setup and Performance Evaluation for LTE-Communications," presented at the *International Workshop on Antenna Technology (iWAT)*, Karlsruhe, Germany, March 2013.
- [32] A. Friedrich, B. Geck, O. Klemp, and H. Kellermann, "On the Design of a 3D LTE Antenna for Automotive Applications based on MID Technology," presented at the *Microwave Conference (EuMC) Proceedings of the 43rd European Conference*, Nuremberg, Germany, Oct. 2013.
- [33] R. Gomez-Villanueva, R. Linares-y-Miranda, J.A. Tirado-Mendez, and H. Jardon-Aguilar, "Ultra-Wideband Planar Inverted-F Antenna (PIFA) for Mobile Phone Frequencies and Ultra-Wideband Applications," *Progress In Electromagnetics Research C*, vol. 43, pp. 109-120, 2013.
- [34] E. Gschwendtner and W. Wiesbeck, "Ultra-Broadband Car Antennas for Communications and Navigation Applications," *IEEE Transactions on Antennas and Propagation*, vol. 51, pp. 2020-2027, Aug. 2003.

**Part II**  
**Included Papers**



# Paper A

## Evaluation of V2X Antenna Performance Using a Multipath Simulation Tool

Edith Condo Neira, Ulf Carlberg, Jan Carlsson, Kristian Karlsson, and Erik G.  
Ström

Published in  
*Proceedings of the 8th European Conference on Antennas and Propagation*  
*(EuCAP)*,  
The Hague, The Netherlands, April 2014  
©2014 IEEE



# Evaluation of V2X Antenna Performance Using a Multipath Simulation Tool

Edith Condo Neira<sup>1</sup>, Ulf Carlberg<sup>1</sup>, Jan Carlsson<sup>1,2</sup>, Kristian Karlsson<sup>1</sup>, Erik G. Ström<sup>2</sup>

<sup>1</sup> SP Technical Research Institute of Sweden, Borås, Sweden, [edith.condoneira@sp.se](mailto:edith.condoneira@sp.se)

<sup>2</sup> Chalmers University of Technology, Gothenburg, Sweden

**Abstract**—Antennas are one of the key components for efficient and reliable vehicular communications systems; especially for safety related applications the antenna performance is crucial. It is therefore important to be able to evaluate the antenna performance under realistic conditions so that the best antenna solution can be selected. In this paper we present a statistical method for evaluating the antenna performance by using the antennas radiation patterns and a multipath simulation tool. The multipath environment is generated by a number of incident waves with a specific angle of arrival distribution, defined by the user. In order to generate voltage samples at the antenna ports many sets of incident waves are generated. This simulates a changing environment as, e.g., when the vehicle is moving. By studying the cumulative distribution functions (CDFs) for the voltage samples we are able to compare the performance for different antenna types, positions on the vehicle, etc. The method is fast and effective and, when applied to typical vehicular propagation environments, the importance of having antennas with radiation patterns capable of covering the whole azimuth plane is demonstrated.

**Index Terms**—V2X Antennas; Measurements; Antenna Performance

## I. INTRODUCTION

In the last few years the interest in vehicle-to-vehicle and vehicle-to-infrastructure communication (together commonly referred to as V2X) has increased significantly. This is mainly due to the many areas of application, such as traffic safety, traffic management and infotainment. In Europe, V2X communications is standardized by ETSI as the ITS-G5 standard [1]. This standard describes a number of safety applications, which require a reliable communication link. In order to achieve such reliable link, antennas with suitable radiation patterns need to be used. The assigned frequency in Europe for vehicle communications is 5.9 GHz and at this high frequency the radiation pattern of an antenna mounted on a vehicle is very complicated with large variations over the solid angle. Thus, it is very difficult to judge which antenna is the best simply by inspecting the radiation pattern.

Many studies have been done in the field of antennas for wireless communications [2]. One example is mobile communications, which in [3], is defined as communication between a fixed base station and a moving user. The base station is normally elevated and the mobile terminal might have any orientation. In this case it is, from the mobile terminal perspective, motivated to study the two extreme environments

random line-of-sight (RLOS) and rich isotropic multipath (RIMP) as was done in [4]. The RLOS is defined as only one incident wave on the terminal, but in order to take the user statistics into account this wave has an arbitrary incidence direction and polarization. In RLOS, we can evaluate the antenna performance by studying the cumulative distribution function (CDF) for the voltage samples at the antenna port that is obtained for many incident waves, i.e., many realizations. In the RIMP environment, which is characterized by many incident waves where the angle-of-arrivals (AoA) of the waves are uniformly distributed over all directions in 3D space, the only antenna parameter of importance is the total radiation efficiency, i.e., the radiation efficiency including the mismatch. In RIMP the CDF for the voltage samples at the antenna port will be Rayleigh distributed independent of the radiation pattern.

For V2X communications on the other hand neither RLOS nor RIMP are relevant. For this case the transmitting as well as the receiving antenna is mounted on roughly the same height and scatterers responsible for the multipath are located mostly in the horizontal plane. This means that waves incident on the receiving antenna will come from arbitrary directions in azimuth but will have a limited angular spread in elevation. For this case, we can talk about richness in the sense that we might have different number of incident waves at a given time or position that together gives the voltage sample at the antenna port. In rural areas and when the two communicating antennas are closely spaced there will often be a dominating line-of-sight (LOS) component and the number of non-line-of-sight components (NLOS) will be few. We simulate this by defining few incident waves when computing the voltage samples. In other types of environments, such as urban or when we have many scattering objects in the vicinity (e.g., in a traffic jam) the number of incident waves might be considerably higher.

Unlike to the situation in RIMP the antenna gain pattern will be important for the overall performance in a typical vehicular communication environment. The question is how to determine which antenna is the best. As is shown in Fig. 1 the radiation patterns for two different 5.9 GHz antennas mounted at the same position on a vehicle are very complicated and it is difficult to judge which one is the best. Thus, it is important to have a good methodology for evaluating the performance of high frequency vehicle antennas that are mounted in different positions and used in different road environments.

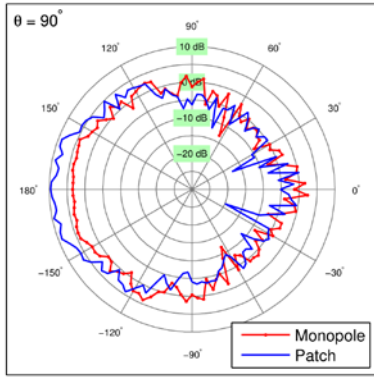


Figure 1. Comparison between the simulated radiation patterns of a quarter-wave monopole and a probe-feed patch antenna mounted on the vehicle's windscreen at 5.9 GHz (elevation plane  $\theta=90^\circ$ ). The front of the vehicle is oriented towards the  $180^\circ$  direction (negative x-axis).

A number of measurement campaigns have been carried out for V2X communications. Some of them have focused on evaluating different positions in which an antenna could be placed [5-7], and others on the evaluation of the channel for different road traffic environments [8]–[9]. The performance considerations of V2V antennas mounted on a vehicle's roof and integrated in an antenna module including other antennas have been evaluated in [10], and [11]. All of these measurements have focused on some specific antenna positions or specific environments. In this paper we focus on the performance of antennas for 5.9 GHz and consider both aspects at the same time, the antenna placement on the vehicle and the road traffic environments.

In this paper we present a method for evaluating the performance of V2X antennas mounted at different positions on a vehicle, and used in different road traffic environments. The method is based on simulations in VIRM-Lab, a computer code which generates a statistically fading environment by a number of statistically varying incoming plane waves [12]. By generating a large number of realizations, each consisting of a number of incident waves on the antenna, the CDF for the voltage at the antenna port is calculated. By comparing the CDFs for different antenna types or positions we are able to determine which configuration will have the best system performance. We simulate different road traffic environments by defining the AoA distribution and the number of waves in each realization.

The paper is organized as follows: In Section II the evaluation method is described and simulations for a few basic antennas are presented. Results for practical antennas mounted on a vehicle are presented in Section III. These results are obtained from simulated as well as measured antenna radiation patterns. Finally, the conclusions are given in Section IV.

## II. ANTENNA EVALUATION METHOD

The evaluation of the antenna performance is done by using the antenna radiation patterns and by simulating the multipath environment. Due to the relative low height in which V2X transmitting and receiving antennas are mounted, multipath phenomena such as scattering, reflections from surrounding buildings and diffraction from other vehicles are expected [13].

As mentioned before, all of these phenomena are located mostly in the horizontal plane. Thus, the incident waves will come from arbitrary directions in azimuth but within a limited range of angles in elevation. Taking this into account and considering the multipath propagation for different road environments, we define the number of incident waves for different cases. For example, for rural areas where there will often be a dominant LOS component and few reflected components [7], the simulation is done by defining few incident waves. For environments such as urban, suburban or highway where there will be more multipath components, a higher number of incident waves are considered in the simulations.

For the simulations, we generate the multipath environment by a number of incident waves, defined by their AoA and polarization. To simulate a changing environment as it is in reality; a large number of realizations are generated, each consisting of a number of statistically distributed incident plane waves, which are distributed statistically on the radiation patterns of the receiving antennas. These incident waves generate a voltage at the antenna ports and then, the CDFs of the received voltages at the antenna ports are calculated. It should be pointed out that the AoA as well as the polarization of the incident waves change for each realization, generating a statistically changing fading signal at the antenna port.

### A. Definition of Weighted Environment for Vehicular Communications

As pointed out before, neither RIMP nor RLOS are typical environments for V2X communications. Therefore, we define the environment for V2X communications as a weighted environment. In the weighted environment the incident waves will come from arbitrary directions in the horizontal plane but within a limited range of angles in elevation. Each wave is linearly polarized with arbitrary polarization. For this environment the CDFs will follow the theoretical Rayleigh as the number of incident waves,  $M$ , increases. However, the CDFs will be shifted to a lower or higher received power level depending on the radiation pattern, showing the dependency of the directivity of the antenna. Notice that the incident waves have random amplitude and phase, being none of them dominant.

TABLE I. Studied Cases for Weighted Environments

Studied Case	Angles	
	<i>Azimuth</i>	<i>Elevation</i>
Case I (uniform)	$0^\circ \leq \phi \leq 360^\circ$	$-5^\circ \leq \theta \leq 15^\circ$
Case II (back)	$-45^\circ \leq \phi \leq 45^\circ$	$-5^\circ \leq \theta \leq 15^\circ$
Case III (front)	$-135^\circ \leq \phi \leq 225^\circ$	$-5^\circ \leq \theta \leq 15^\circ$

Three different environments have been studied, see Table I. Road environments like highway or urban might be represented by Case I. This case represents an environment in which the incident waves are coming uniformly distributed in the azimuth plane with a certain angle of elevation distribution. Case II and Case III; represent an environment where the waves are incident on either the front ( $\phi = 180^\circ$ ) or the rear ( $\phi$

$= 0^\circ$ ) of the vehicle defined by a  $90^\circ$  sector in azimuth. This might be the case in a rural environment. For all cases, the incident waves are uniformly distributed in azimuth as well as in elevation in the intervals specified in Table I. When computing the CDFs, we have used  $10^5$  realizations. Each realization contains one and twenty linearly polarized incident waves with random polarization, respectively. The AoA as well as the polarization of each incident wave are statistically independent. The phase of the incident waves are uniformly distributed between 0 and  $2\pi$  radians and the amplitude is Rayleigh distributed. In the figures to follow, the average power has been normalized to one.

### B. Performance for Basic Antennas in Weighted Environment

Three basic 5.9 GHz antennas, a dipole, a quarter-wave monopole centricly mounted on a ground plane with size of  $1 \times 1 \text{ m}^2$ , and a patch antenna, have been evaluated. For the evaluation, calculated antenna radiation patterns in free space have been used. As can be seen in Fig. 2-4, the CDFs for the dipole antenna show pretty much the same results for the three studied cases. For the quarter-wave monopole antenna, the CDFs for the three studied cases are also very similar. This is because the monopole antenna has a similar radiation pattern compared to the dipole in the range of angles defined by the environments.

The patch antenna is probe-feed and has a length of 11 mm, width of 15 mm and a ground plane size of  $20 \times 24 \text{ mm}$ . The substrate is FR4 with a thickness of 1.6 mm. Since the patch is a directional antenna, the CDF changes according to the environment in which it is simulated. In Fig. 3, the incident waves are coming from the opposite direction compared to the patch main beam; this will of course have a negative effect on the performance. However, when the incident waves are coming from the same direction as the patch main beam, the antenna will perform much better than the dipole and the monopole antenna, see Fig. 4.

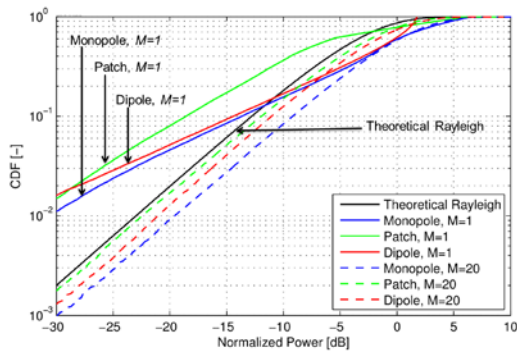


Figure 2. CDFs for linear polarized incident waves. Solid lines represent a weighted RLOS environment ( $M=1$ ) and dashed lines represent a weighted environment ( $M=20$ ). The simulations are done for Case I (see Table I). The Patch antenna is radiating towards the negative x-axis.

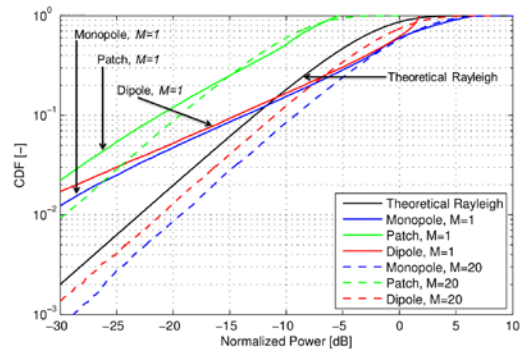


Figure 3. CDFs for linear polarized incident waves. Solid lines represent a weighted RLOS environment ( $M=1$ ) and dashed lines represent a weighted environment ( $M=20$ ). The simulations are done for Case II (see Table I). The Patch antenna is radiating towards the negative x-axis. The opposite direction in which the incident waves are coming.

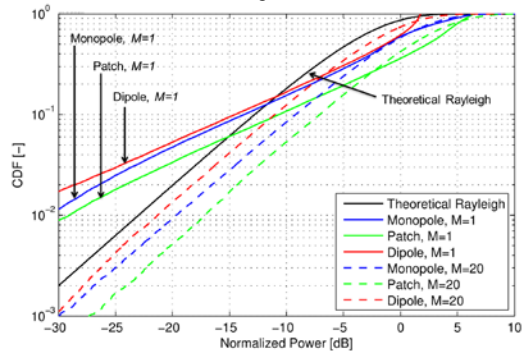


Figure 4. CDFs for linear polarized incident waves. Solid lines represent a weighted RLOS environment ( $M=1$ ) and dashed lines represent a weighted environment ( $M=20$ ). The simulations are done for Case III (see Table I). The Patch antenna is radiating towards the negative x-axis. The same direction in which the incident waves are coming.

## III. RESULTS FOR PRACTICAL ANTENNAS

A few basic antennas were manufactured and the radiation patterns for the antennas mounted on a vehicle in a few different positions were both simulated and measured. The simulations were done in CST Microwave Studio and the measurements were done in a semi-anechoic chamber. For both simulations and measurements, the antennas were mounted on two different positions on the vehicle, the windscreen and the rear window, respectively. The vehicle was aligned along the x-axis with the front pointing in the negative x-axis direction, as shown in Fig. 5. The practical antennas were a quarter-wave monopole and a probe-feed patch antenna, both of them resonating at 5.9 GHz. The monopole was mounted in the center of a ground plane with size of  $30 \times 30 \text{ mm}^2$ . The dimensions of the patch antenna were the same as defined in the previous section.

In this section, we have only used vertically polarized incident waves since the two manufactured antennas were vertically polarized. The CDFs are generated from the simulated and measured antenna radiation patterns and a defined weighted environment. For all cases, the CDFs were computed with  $10^5$  realizations. Each realization contains one and twenty vertically polarized incident waves, respectively.

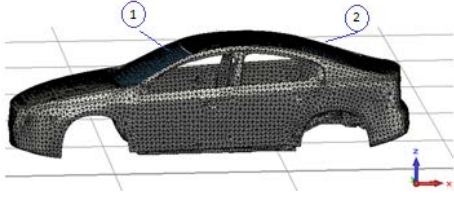


Figure 5. Orientation of the vehicle. The antennas are mounted in two different positions; (1) Windscreen and (2) rear window.

### A. Performance for Simulated Antennas

The CDFs for the monopole and patch antennas are shown in Fig. 6. Both antennas are mounted on the windscreen of the vehicle and the vertically polarized incident waves are coming as defined by Case I (see Table I). In this case, we can see that the patch antenna performs better than the monopole when we have twenty vertical polarized incident waves in each realization. However, when we only have one wave in each realization the monopole antenna performs better, except at high levels where the patch becomes better again. This behavior can be understood by analyzing the radiation patterns shown in Fig. 1 where it can be seen that the monopole has a smoother radiation pattern in azimuth and the patch has a higher directivity as well as deeper dips in the pattern.

In Fig. 7, the vertical incident waves are coming as defined by Case III (see Table I). As can be seen, the patch antenna performs much better than the monopole in this case. This is because the incident waves are coming from the same direction in which the patch is radiating, i.e., toward the front of the vehicle. However, when the vertical incident waves are coming from the opposite side in which the patch is radiating, i.e., incident waves on the rear of the vehicle, the monopole performs better than the patch. By comparing Fig. 7 and Fig. 8 we can as expected see that when the antennas are mounted on the windscreen they both perform much better when the waves are incident on the front of the vehicle as compared to the rear. We can also note that the difference between the two antenna types is large when the waves are incident on the front while the difference is smaller when the waves are incident on the rear of the vehicle.

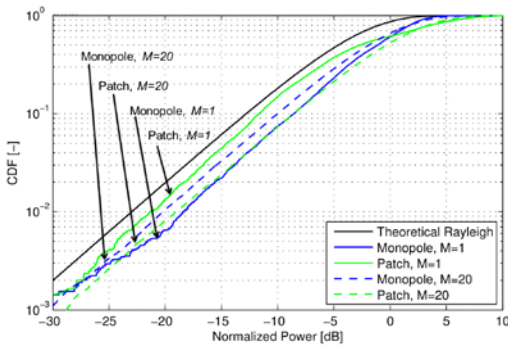


Figure 6. CDFs for vertical polarized incident waves. Solid lines represent a weighted RLOS environment ( $M=1$ ) and dashed lines represent a weighted environment ( $M=20$ ). The simulations are done for Case I (see Table I). The Patch antenna is radiating towards the negative x-axis. The antennas are mounted on the vehicle's windscreen.

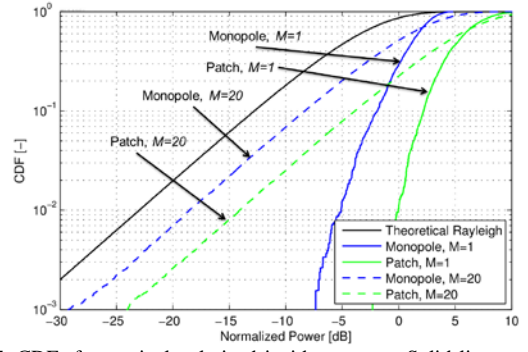


Figure 7. CDFs for vertical polarized incident waves. Solid lines represent a weighted RLOS environment ( $M=1$ ) and dashed lines represent a weighted environment ( $M=20$ ). The simulations are done for Case III (see Table I). The Patch antenna is radiating in the direction in which the incident waves are coming. The antennas are mounted on the vehicle's windscreen.

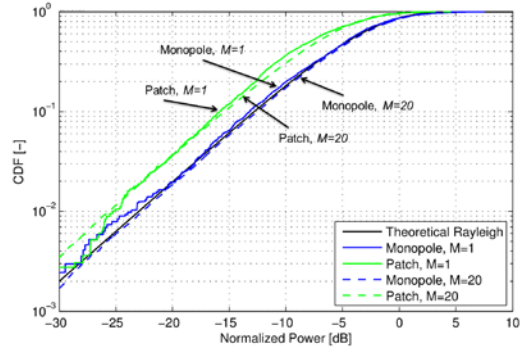


Figure 8. CDFs for vertical polarized incident waves. Solid lines represent a weighted RLOS environment ( $M=1$ ) and dashed lines represent a weighted environment ( $M=20$ ). The simulations are done for Case II (see Table I). The Patch antenna is radiating in the opposite direction in which the incident waves are coming. The antennas are mounted on the vehicle's windscreen.

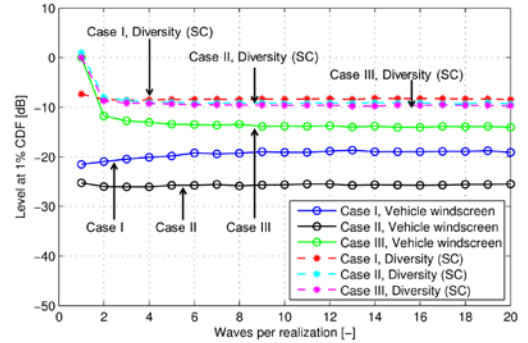


Figure 9. Received power at 1% CDF-level as a function of vertical polarized incident plane waves. The simulations are done for the three studied cases (see Table I) when the patch is mounted on the vehicle's windscreen. The graph also shows the diversity combined results for the three studied cases when one patch is mounted on the vehicle's windscreen and another one on the rear window.

In Fig. 9, we can see the difference between the three studied cases (see Table I) when the patch antenna is mounted on the windscreen of the vehicle. We can see that the patch performs best in Case III and this is because the vertical incident waves are coming from the same direction in which the patch is radiating, i.e., toward the front of the vehicle. With this knowledge, we can use diversity to improve signal quality. This is also shown in Fig. 9, where selection combining (SC) was used to combine signals from patch antennas mounted on the vehicle's windscreen and rear window, respectively.

## B. Performance for Measured Antennas

The radiation pattern measurements were done in a semi-anechoic chamber which had a solid metallic floor temporary filled with absorbers. The probe-feed patch antennas were mounted on the vehicle's windscreen and on the rear window. To perform the measurements, a turntable was used to collect the data every two degrees in the azimuth plane (full 360°), and a mast to collect the measurement data for few angles in the elevation plane.

In Fig. 10, the CDFs results for the antenna mounted on both positions are shown. The incident waves are coming as in Case I (see Table I). As can be seen, when we have twenty vertical polarized incident waves, the patch mounted on the vehicle's windscreen performs better than when mounted on the vehicle's rear window.

## C. Comparison Between Simulated and Measured Antennas

In order to compare simulations with measurements, we have studied the patch antenna mounted on the vehicle's windscreen. The comparison was done for Case I (see Table I). In Fig. 11, it can be seen that the CDFs results for both the simulated and the measured radiation patterns follow the theoretical Rayleigh when we have twenty vertical incident waves. However, the measured radiation pattern is slightly better than the simulated.

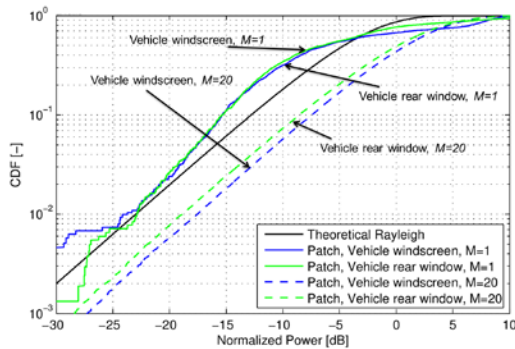


Figure 10. CDFs for vertical polarized incident waves. Solid lines represent a weighted RLOS environment ( $M=1$ ) and dashed lines represent a weighted environment ( $M=20$ ). The simulations are done for Case I (see Table I). The patch is mounted in the vehicle's windscreen and rear window.

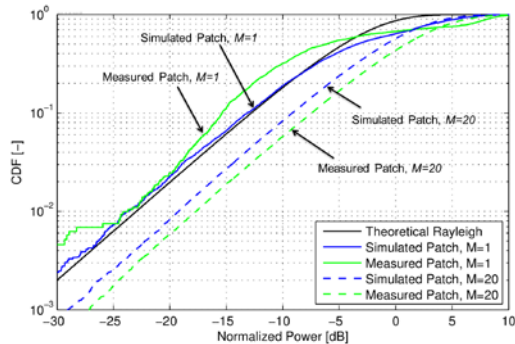


Figure 11. CDFs for vertical polarized incident waves. Solid lines represent a RLOS environment ( $M=1$ ) and dashed lines represent a weighted environment ( $M=20$ ). The simulations are done for Case I (see Table I).

## IV. CONCLUSION

We have presented a method for evaluating the performance of V2X antennas mounted at different positions and used in different road traffic environments. Simulations and measurement results performed on the vehicle emphasize the importance of antennas with radiation patterns covering the whole azimuth plane. The statistical method that we have presented is fast, effective and in general give us a good idea of a suitable antenna placement on vehicle, the type and the number of antennas that are needed in a real environment.

## ACKNOWLEDGMENT

This work has been supported by The Swedish Governmental Agency for Innovation Systems (VINNOVA) within the VINN Excellence Center Chase.

## REFERENCES

- [1] E. G. Ström, "On Medium Access and Physical Layer Standards for Cooperative Intelligent Transport Systems in Europe," *Proceedings of the IEEE*, vol. 99, no. 7, pp. 1183-1188, July 2011.
- [2] A.M.Yadav, C.J.Panagamuwa, and R.D.Seager, "A Miniature Reconfigurable Printed Monopole Antenna for WLAN/WiMAX and LTE Communication Bands," *Loughborough Antennas & Propagation Conference (LAPC)*, Loughborough, UK, Nov. 2013.
- [3] K. Fujimoto and J. R. James, *Mobile Antenna Systems Handbook*, Second ed. Norwood, MA, USA: Artech House, 2001.
- [4] J. Carlsson, U. Carlberg, and P. S. Kildal, "Diversity Gains in Random Line-Of-Sight and Rich Isotropic Multipath Environment," *Loughborough Antennas & Propagation Conference (LAPC)*, Loughborough, UK, Nov. 2012.
- [5] L. Reichardt, T. Fügen, and T. Zwick, "Influence of Antennas Placement on Car to Car Communications Channel," *Antennas and Propagation (EuCAP), Proceedings of the 3rd European Conference*, Berlin, Germany, Mar. 2009.
- [6] S. Kaul, K. Ramachandran, P. Shankar, S. Oh, M. Gruteser, I. Seskar, and T. Nadeem, "Effect of Antenna Placement and Diversity on Vehicular Network Communications," *Sensor, Mesh and Ad Hoc Communications and Networks (SECON)* pp. 112-121, June 2007.
- [7] T. Abbas, J. Karedal, and F. Tufvesson, "Measurement-Based Analysis: The Effect of Complementary Antennas and Diversity on Vehicle-to-Vehicle Communication," *IEEE Antennas and Wireless Propagation Letters*, vol. 12, pp. 309-312, Mar. 2013.
- [8] J. Kunisch and J. Pamp, "Wideband Car-to-Car Radio Channel Measurements and Model at 5.9 GHz," in *IEEE Vehicular Technology Conference. VTC 2008-Fall*, Calgary, Canada, Sept. 2008.
- [9] R. Protzmann, B. Schünemann, and I. Radusch, "The Influences of Communication Models on the Simulated Effectiveness of V2X Applications," *IEEE Commun. Magazine* pp. 149-155, Nov. 2011.
- [10] O. Klemp, "Performance Considerations for Automotive Antenna Equipment in Vehicle-to-Vehicle Communications," *URSI International Symposium on Electromagnetic Theory*, pp. 934-937, Aug. 2010.
- [11] M. Gallo, S. Bruni, M. Pannozzo, and D. Zamberlan, "Performance Evaluation of C2C antennas on Car Body," *Antennas and Propagation (EuCAP) Proceedings of the 7th European Conference*, Gothenburg, Sweden, April 2013.
- [12] U. Carlberg, J. Carlsson, A. Hussain, and P. S. Kildal, "Ray Based Multipath Simulation Tool for Studying Convergence and Estimating Ergodic Capacity and Diversity Gain for Antennas with Given Far-Field Functions," in *20th Internat. Conf. on Applied Electromagnetics and Communications (ICECom)*, Dubrovnik, Croatia, Sept. 2010.
- [13] B. Gallagher and H. Akatsuka, "Wireless Communications for Vehicle Safety: Radio Link Performance and Wireless Connectivity Methods," *IEEE Vehicular Technology Magazine*, pp. 4-24, Dec. 2006.



# Paper B

## Combined LTE and IEEE 802.11p Antenna for Vehicular Applications

Edith Condo Neira, Jan Carlsson, Kristian Karlsson, and Erik G. Ström

Published in  
*Proceedings of the 9th European Conference on Antennas and Propagation*  
*(EuCAP)*,  
Lisbon, Portugal, April 2015  
©2015 IEEE



# Combined LTE and IEEE 802.11p Antenna for Vehicular Applications

Edith Condo Neira<sup>1</sup>, Jan Carlsson<sup>1</sup>, Kristian Karlsson<sup>1</sup>, Erik G. Ström<sup>2</sup>

<sup>1</sup> SP Technical Research Institute of Sweden, Borås, Sweden, edith.condoneira@sp.se

<sup>2</sup> Chalmers University of Technology, Gothenburg, Sweden

**Abstract**—Vehicles may contain multiple antennas for different applications. Among all of them, Vehicle-to-Vehicle and Vehicle-to-Infrastructure (V2X) is one of the most recent applications. This new technology focuses on traffic safety and traffic efficiency. In this paper we present a new compact antenna module suitable for vehicular applications. This module could be easily integrated into the rear-spoiler on a vehicle. The module consists of two identical monopoles for V2X applications based on the IEEE 802.11p standard and two identical printed inverted F-antennas for Long-Term Evolution (LTE) communications. The evaluation of the proposed module is done by analyzing the simulated and measured antenna S-parameters, antenna efficiencies, radiation patterns, as well as by calculating the diversity performance. The results show that the antennas are well matched and well isolated for both LTE and V2X and exhibits a radiation pattern close to the desired omnidirectional in the horizontal plane for V2X. The two LTE antennas have radiation patterns that complement each other ensuring an omnidirectional coverage by combination. Furthermore the module presents good radiation efficiency for both LTE and V2X.

**Index Terms**—Antenna Module; LTE and V2X antennas; LTE and 802.11p antennas; Vehicular Antennas.

## I. INTRODUCTION

In the last few years, the automotive industry has increased its interest in wireless technologies significantly. It is well known that antennas are key components to assure a reliable wireless communications link. Modern vehicles may contain multiple antennas covering different frequency bands for different wireless applications. In addition to the existing applications, modern vehicles will include Long-Term Evolution (LTE) and Vehicle-to-Vehicle and Vehicle-to-Infrastructure (V2X) technologies. LTE will provide high data rates for several applications such as Internet connectivity. V2X, which is currently based on IEEE 802.11p, will allow vehicles to communicate with each other and with the road infrastructure improving traffic safety and traffic efficiency. In Europe, IEEE 802.11p is used as basis for the ITS-G5 standard which is standardized by European Telecommunications Standard Institute (ETSI) with a bandwidth allocation of 30 MHz at 5.9 GHz (i.e., from 5875 MHz to 5905 MHz) [1]. The increasing number of antennas and the restricted space due to aesthetic aspects requires the development of multiband antennas integrated in a single compact module that preferably should be placed hidden in some part (e.g., a spoiler) of the vehicle.

Therefore, a lot of research is conducted on designing antennas capable of covering different frequency bands and fitted in the same module [2-4]. Most of them have focused on some specific technology. For example the design and performance of LTE antennas were presented in [5] while [6] proposed a module including antennas for V2V communications. In [7], a module including V2V as well as LTE antennas was published. All of these modules have been proposed for a roof-top mounting position. To the authors' best knowledge there is no published information about other mounting positions regarding antennas for LTE and V2X technologies.

This paper describes the design and performance evaluation of a compact module consisting of diversity antennas for LTE and V2X technologies. The module is proposed to be mounted inside the rear-spoiler and it consists of two identical LTE antennas covering the frequency bands specified in Table I, and two identical V2X antennas for 5.9 GHz. The LTE antennas are based on a printed inverted F-antenna (PIFA) design [8], to which a slot has been added to increase the bandwidth and to achieve good performance in the lowest LTE band specified in Table I. The V2X antennas are quarter-wave monopoles. For the evaluation, we measure the S-parameters, the radiation efficiency as well as the total radiation efficiency, and the radiation patterns.

We also investigate diversity taking into account the multipath environment to which vehicles are exposed. This is done by using the radiation patterns and a statistical method [9] which is based on simulations in VIRM-Lab, a computer code for analyzing the performance of multipoint antennas in multipath environments [10]. The multipath environment is generated by a number of incident waves with a specific angle of arrival distribution, defined by the user. The incident waves will generate a voltage at the antenna ports. By generating several sets of waves and studying the received power at 1% Cumulative Distribution Function (CDF)-level and by applying diversity techniques we are able to characterize the performance of the antenna module.

The paper is organized as follows: In Section II the design for LTE and V2X antennas is described as well as the antenna module design. In Section III, the evaluation of the antenna module is presented. This includes the antenna S-parameters, antenna efficiencies, radiation patterns as well as the received power at 1% CDF-level when using selection diversity combination. Finally, the conclusions are given in Section IV.

## II. MULTI-FUNCTION ANTENNA

The multi-function antenna module is designed to be within the dimensions of 300 mm length, 50 mm width and 20 mm height. This is considering the available space inside the rear-spoiler on a vehicle, e.g., a crossover vehicle.

### A. Antenna Design

Fig. 1 shows the geometry of the proposed antennas for LTE as well as for V2X communications. As mentioned before the LTE antenna is based on a PIFA design [8]. The antenna consists of a radiating element, a shorting strip, a feeding element, and a ground plane. The radiating element is shorted to the ground plane by the shorting strip as in any conventional PIFA design. The height between the ground plane and the radiating element is 5 mm. In order to allow a better current distribution a wide feeding element is used. As shown in Table I, the lowest frequency band is between 698 MHz to 716 MHz. At these frequencies the ground plane is the main contributor to the radiation, which means that the size of the ground plane should be in the order of half wavelength, i.e., in the order of 200 mm, for good radiation performance. Thus, we need to make the ground plane sufficiently large electrically and at the same time keep the physical length small due to the limited available space. We achieve this by inserting three slots in the ground plane. Two of the slots are placed under the radiating element followed by the third one that is placed further out on the ground plane. The slots have a length of 5 mm and a width of 26 mm. The dimensions of the PIFA are given in Table II.

For V2X communications a quarter-wave length monopole antenna is used. The antenna resonates at 5.9 GHz and it is mounted on the PIFA ground plane as shown in Fig. 1.

Table I. Frequency Bands for LTE

LTE Frequency Bands	
Uplink	Downlink
698 - 716 MHz	925 - 960 MHz
1710 - 1785 MHz	2110 - 2170 MHz
2500 - 2570 MHz	2620 - 2690 MHz

Table II. Dimensions of PIFA for LTE Communications

Description	Dimensions
Radiating element	Length = 25 mm; Width = 40 mm; Thickness = 1 mm
Feeding element	Height = 4 mm; Width = 17 mm; Thickness = 1 mm
Shorting strip	Height = 5 mm; Width = 1 mm; Thickness = 1 mm
Ground Plane	Length = 120 mm; Width = 40 mm; Thickness = 0.1 mm



Figure 1. PIFA antenna for LTE Communications including a quarter-wave length monopole.

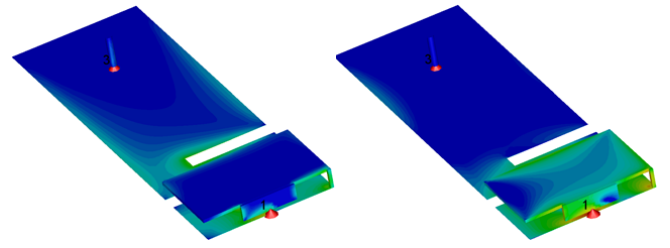


Figure 2. Current distribution at 698 MHz (left) and 2690 MHz (right).

Fig. 2 shows the surface current at 698 MHz and 2690 MHz which are the lowest and highest frequencies for LTE, see Table I. It is shown that at lower frequencies the main contributor to radiation is the ground plane while at higher frequencies the main contributor is the radiating element.

### B. Final Antenna Module Design

Two identical LTE and two identical V2X antennas are used in the antenna module. The LTE antennas are printed on FR4 substrate with permittivity of 4.3, loss tangent of 0.025, and thickness of 1.6 mm, and each of them has its own ground plane, which are spatially separated by 50 mm. This is done to achieve a good isolation between the antennas as well as to have enough space for future GPS antenna integration. For V2X, the antennas are mounted on the ground plane of each LTE antenna and the separation between them is 90 mm. The design and optimization of the antenna module is done in CST Microwave Studio [11]. The complete module has a length of 290 mm, width of 40 mm, and a height of 7.6 mm. The final antenna module prototype is shown in Fig. 3. For the measurements, the feeding of the antennas is made through a 50  $\Omega$  SMA connector. The manufactured antenna module is shown in Fig. 4.

## III. EVALUATION OF THE ANTENNA MODULE

The antenna module has been both simulated and measured. For convenience the antennas are referred to as antenna 1 and 2 for LTE and antenna 3 and 4 for V2X as shown in Fig. 3.

### A. Analysis of S-parameters

The simulations were done in CST Microwave Studio and for the measurements a vector network analyzer was used.

In Fig. 5 and Fig. 6, the simulated and measured return losses ( $-S_{ii}$ ) of the antenna module are shown. As can be seen in Fig. 5, the return loss for LTE antennas is better than 6 dB in all relevant frequency bands specified in Table I. The difference between the simulated and measured LTE antennas as well as the difference between both measured LTE antennas is attributed to factors such as manual soldering and manufacturing tolerances. For V2X, the antennas are well matched at 5.9 GHz. Both the simulated and measured return loss is better than 13 dB, see Fig. 6.

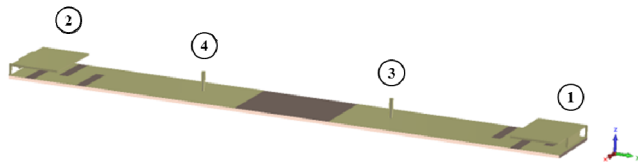


Figure 3. Antenna module for LTE and V2X communications.



Figure 4. Fabricated prototype of the antenna module

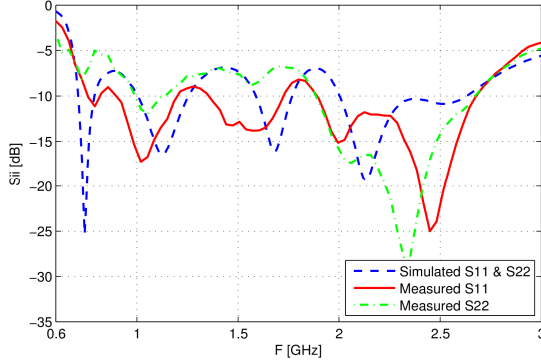


Figure 5. Simulated and measured return loss of the antenna module for LTE antennas.

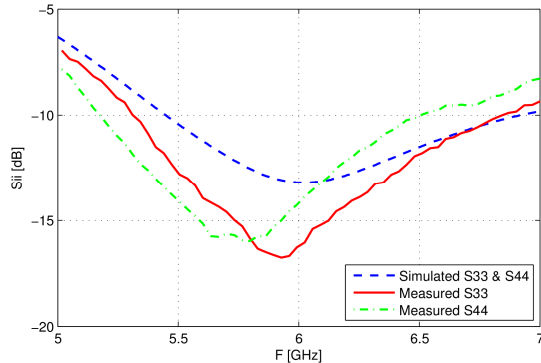


Figure 6. Simulated and measured return loss of the antenna module for V2X antennas.

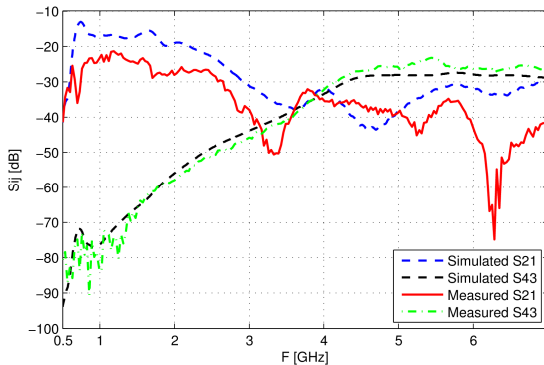


Figure 7. Simulated and measured mutual coupling between antenna 1 and 2 (LTE antennas) and between antenna 3 and 4 (V2X antennas).

As mentioned before the distance between the antennas were optimized to achieve good isolation. The resulting isolation is shown in Fig. 7 and Fig. 8. In Fig. 7, the mutual coupling between the LTE antennas (S21) is less than  $-15$  dB at the lower bands and less than  $-20$  dB at the

highest band specified in Table I. For V2X the mutual coupling between the antennas (S43) is less than  $-26$  dB. The mutual coupling between the LTE antenna 1 and V2X antenna 3 (S31) is less than  $-20$  dB and less than  $-30$  dB between LTE antenna 2 and V2X antenna 3, as shown in Fig. 8.

The measured radiation efficiency as well as the total radiation efficiency for LTE antennas is shown in Fig. 9. As can be seen the total radiation efficiency is better at the highest band in comparison to the lower bands. This is due to the antenna is better matched at higher frequencies. For V2X, the difference between the radiation efficiency and the total radiation efficiency is less than  $0.2$  dB, see Fig. 10. This is because the antennas are well matched.

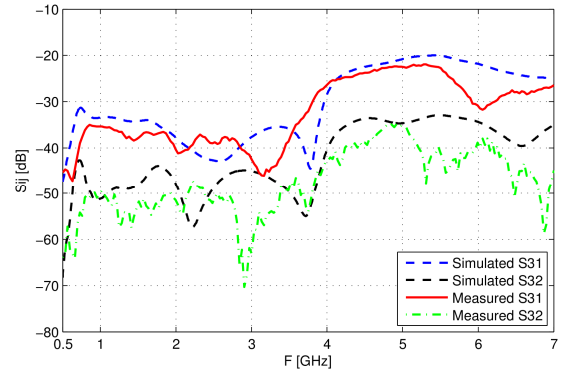


Figure 8. Simulated and measured mutual coupling between antenna 1 (LTE) and 3 (V2X) and between antenna 2 (LTE) and 3 (V2X).

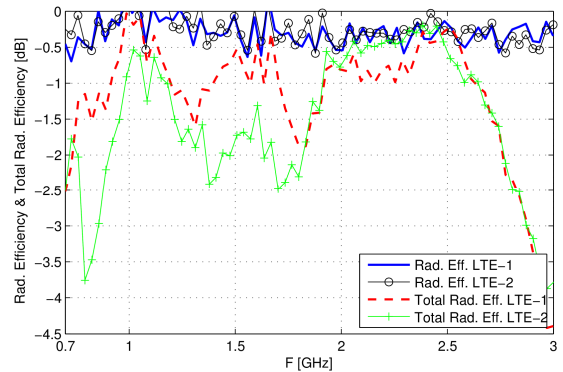


Figure 9. Measured radiation efficiency and total radiation efficiency for the LTE antennas.

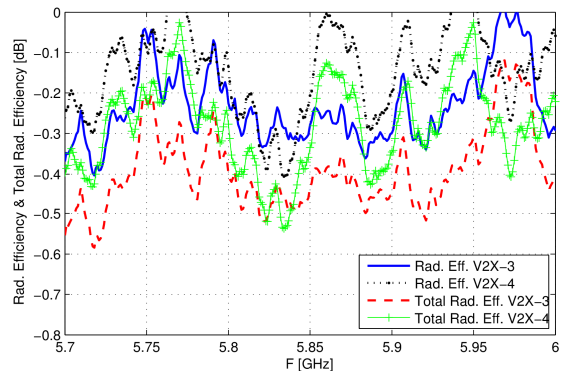


Figure 10. Measured radiation efficiency and total radiation efficiency for the V2X antennas.

### B. Analysis of Radiation Patterns

The radiation pattern measurements were done in an anechoic chamber.

The measured radiation patterns at three different frequencies of 829 MHz, 1940 MHz, and 2590 MHz are shown in Fig. 11. These frequencies are the center frequencies of the LTE bands specified in Table I. As can be seen, the two LTE antennas have radiation patterns that complement each other, at least for the higher frequency bands. Thus, combined, they are close to omnidirectional in the azimuth plane. Fig. 12 shows the measured radiation pattern at 5.9 GHz. As expected, the radiation pattern is close to omnidirectional in the azimuth plane.

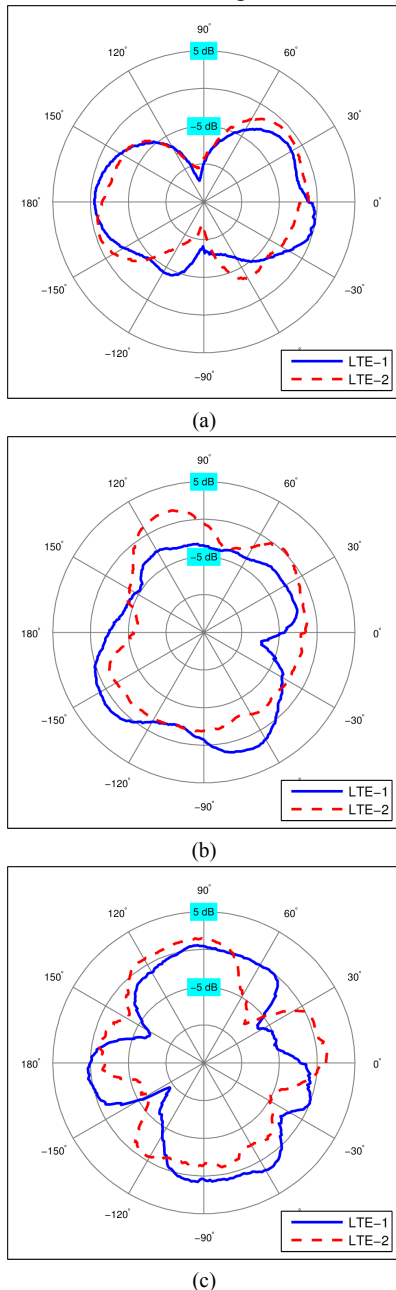


Figure 11. Measured radiation patterns (total gain) for LTE in the azimuth plane. (a) 830 MHz, (b) 1940 MHz, (c) 2590 MHz.

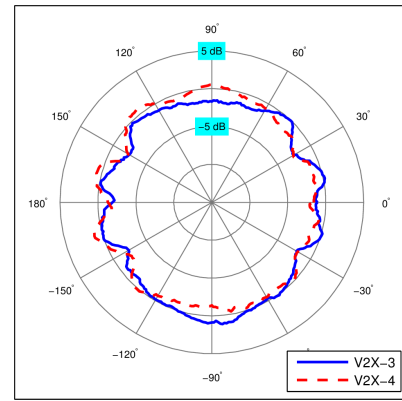


Figure 12. Measured radiation pattern (total gain) for V2X in the azimuth plane.

### C. Received Power at 1% CDF-level

As was done in [9], we here assume the multipath phenomena for V2X communications to be located mostly in the horizontal plane. Thus, the incident waves will come within a limited range of angles in elevation and from arbitrary directions in azimuth. The incident waves are uniformly distributed in both elevation and azimuth.

For the simulations, we generate the multipath environment by a number of incident waves, defined by their angle of arrival and polarization. In order to resemble reality, a large number of realizations are generated to simulate a changing environment when computing the received power at 1% CDF-level. Each realization consists of a number of statistically distributed incident plane waves, which are distributed on the radiation patterns of the receiving antennas. These incident waves generate a voltage at the antenna ports.

In the figures to follow, we have used  $10^5$  realizations and each realization contains two to twenty incident plane waves. The incident waves are uniformly distributed between  $0^\circ$  to  $360^\circ$  in azimuth and  $-5^\circ$  to  $15^\circ$  in elevation. The phase of the incident waves are uniformly distributed between 0 and  $2\pi$  radians and the amplitude is Rayleigh distributed. In order to give a feeling for the performance of our antennas, an ideal half-wave vertical dipole is used for comparison.

For LTE, we have used linearly polarized incident waves with random polarization since the antennas for LTE base stations are dual-polarized. Fig. 13 shows the results for LTE at three different frequencies. As can be seen, the LTE antennas are better than the dipole antenna for all the studied frequencies. It is also shown in the graphs that the signal quality can be improved by applying diversity selection combining. The signal quality at 829 MHz, 1940 MHz and 2590 MHz improves around 3.1 dB, 4.5 dB and 5 dB, respectively.

In Fig. 14, the results for V2X are shown. Here, we have only used vertically polarized incident waves. This is because the manufactured V2X antennas are vertically polarized and we assume the opposite side of the link to have the same polarization. As expected, the received power at

1% CDF-level is better than the dipole antenna. Applying diversity selection combining improves signal quality around 2.4 dB.

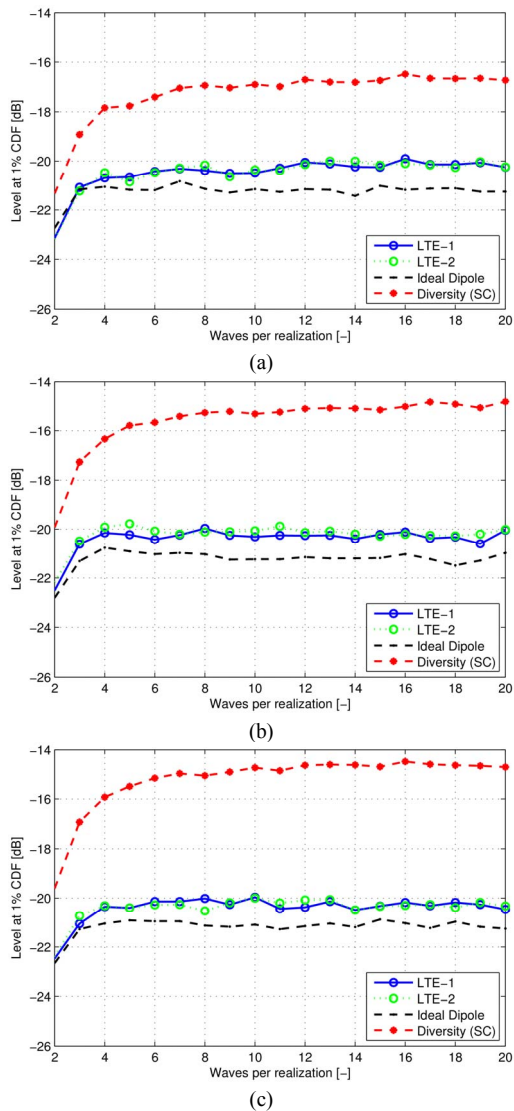


Figure 13. Received power at 1% CDF-level as a function of linearly polarized incident waves for LTE at three different frequencies. (a) 830 MHz, (b) 1940 MHz, (c) 2590 MHz. Diversity selection combining is also shown in the graph.

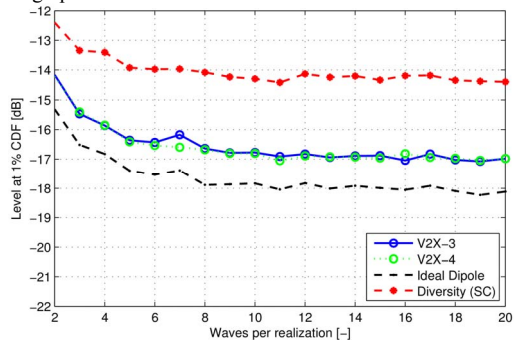


Figure 14. Received power at 1% CDF-level as a function of vertical polarized incident waves for V2X, i.e., 5.9 GHz. Diversity selection combining is also shown in the graph.

#### IV. CONCLUSION

We have presented a compact module consisting of two identical LTE and two identical V2X antennas. The overall size of the module is  $290 \times 40 \times 7.6 \text{ mm}^3$  and it is suitable for a rear-spoiler mounting position. Simulations and measurements results performed on the module show that the antennas are well matched and well isolated for the three different studied LTE frequency bands as well as for V2X communications. Moreover the module presents a total radiation efficiency of  $-1.5 \text{ dB}$  at the lowest band,  $-1.2 \text{ dB}$  at the middle band and  $-0.8 \text{ dB}$  at the highest band for LTE and  $-0.5 \text{ dB}$  for V2X.

#### ACKNOWLEDGMENT

This work has been supported by The Swedish Governmental Agency for Innovation Systems (VINNOVA) within the VINN Excellent Center Chase.

#### REFERENCES

- [1] E. G. Ström, "On Medium Access and Physical Layer Standards for Cooperative Intelligent Transport Systems in Europe" *Proceedings of the IEEE*, vol. 99, no. 7, pp. 1183-1188, July 2011.
- [2] B. Sanz-Izquierdo and R. Leelaratne, "Evaluation of Wideband LTE Antenna Configurations for Vehicular Applications," *Loughborough Antennas & Propagations Conference (LAPC)*, Loughborough, UK, Nov. 2013.
- [3] E. Gschwendtner and W. Wiesbeck, "Ultra-Broadband Car Antennas for Communications and Navigation Applications," *IEEE Transactions on Antennas and Propagation*, vol. 51, pp. 2020-2027, Aug. 2003.
- [4] R. Leelaratne and R. Langley, "Multiband PIFA Vehicle Telematics Antennas" *IEEE Transactions on Vehicular Technology*, vol. 54, pp. 477-485, March 2005.
- [5] A. Thiel, L. Ekiz, O. Klemp, and M. Schutz, "Automotive Grade MIMO Antenna Setup and Performance Evaluation for LTE-Communications," *International Workshop on Antenna Technology (iWAT)*, Karlsruhe, Germany, March 2013.
- [6] M. Gallo, S. Bruni, and D. Zamberlan, "Design and Measurement of Automotive Antennas for C2C Applications," *Antennas and Propagation (EuCAP) Proceedings of the 6th European Conference*, Prague, Czech Republic, March 2012.
- [7] M. Gallo, S. Bruni, M. Pannozzo, and D. Zamberlan, "Performance Evaluation of C2C Antennas on Car Body," *Antennas and Propagation (EuCAP) Proceedings of the 7th European Conference*, Gothenburg, Sweden, April 2013.
- [8] R. Gomez-Villanueva, R. Linares-y-Miranda, J.A. Tirado-Mendez, and H. Jardón-Aguilar, "Ultra-Wideband Planar Inverted-F Antenna (PIFA) for Mobile Phone Frequencies and Ultra-Wideband Applications," *Progress In Electromagnetics Research C*, vol. 43, pp. 109-120, 2013.
- [9] E. Condo Neira, U. Carlberg, J. Carlsson, K. Karlsson, and E. G. Ström, "Evaluation of V2X Antenna Performance Using a Multipath Simulation Tool," *Antennas and Propagation (EuCAP) Proceedings of the 8th European Conference*, The Hague, The Netherlands, April 2014.
- [10] U. Carlberg, J. Carlsson, A. Hussain, and P. S. Kildal, "Ray Based Multipath Simulation Tool for Studying Convergence and Estimating Ergodic Capacity and Diversity for Antennas with Given Far-Field Functions," in *20th Internat. Conf. on Applied Electromagnetics and Communications (ICECom)* Dubrovnik, Croatia, Sept. 2010.
- [11] *CST Microwave Studio*. Available: <https://www.cst.com/>



# Paper C

## V2V Antenna Evaluation Method in a Simulated Measurement-Based Multipath Environment

Edith Condo Neira, Kristian Karlsson, Erik G. Ström, Jan Carlsson, and Amir  
Majidzadeh

Submitted to  
*IEEE Transaction on Antennas and Propagation*,  
Dec. 2016



# V2V Antenna Evaluation Method in a Simulated Measurement-Based Multipath Environment

Edith Condo Neira<sup>1</sup>, Kristian Karlsson<sup>1</sup>, Erik G. Ström<sup>2</sup>, Jan Carlsson<sup>2,3</sup>, Amir Majidzadeh<sup>4</sup>

<sup>1</sup> SP Technical Research Institute of Sweden, Borås, Sweden, edith.condoneira@sp.se

<sup>2</sup> Chalmers University of Technology, Gothenburg, Sweden

<sup>3</sup> Provinn AB, Gothenburg, Sweden

<sup>4</sup> Volvo Car Corporation, Gothenburg, Sweden

**Abstract**—In this paper, we present an efficient method for evaluating Vehicle-to-Vehicle (V2V) antenna performance in multipath environments. In a V2V scenario, the angular received power spectrum depends on the environment (urban, rural, highway, etc.). We propose to characterize the environment by the relative received power in four equal-sized sectors (front, left, back, right). The environment parameters, which we acquire in a measurement campaign, are used to create a simulated multipath environment in which V2V antenna patterns are readily evaluated in terms of the received power cumulative distribution functions (CDFs). The method is validated by comparing the simulated and measured received power for two roof-top vehicle antennas, and the results indicate that the method is quite accurate. Moreover, given the environment parameters, the method is quite fast and efficient.

**Index Terms**—Antenna Evaluation, V2V Measurements, V2V Simulations, Multipath.

## I. INTRODUCTION

In recent years, there has been a considerable interest from the automotive industry in implementing more and more wireless technologies in the vehicles. One of the most recent and fast growing wireless technology is Vehicle-to-Vehicle (V2V) communication, which in Europe is standardized by ETSI as the ITS-G5 standard, and in the United States the standard is called DSRC. Both ITS-G5 [1] and DSRC [2] rely on the PHY and MAC layers of IEEE 802.11p and they operate in the 5.9 GHz band. V2V main focus is on traffic safety and traffic efficiency. For traffic safety applications, it is of utmost importance that the wireless link is reliable in different V2V propagation environments. Antenna performance is crucial for reliability, and it is therefore important to find accurate and efficient methods for antenna performance evaluation in realistic propagation environments.

For V2V communications the transmitting as well as the receiving antennas are mounted roughly on the same height and scatterers responsible for the multipath are located mostly in the horizontal plane. Thus, the waves that are incident on the receiving antenna will come from arbitrary directions in azimuth but within a limited range of angles in elevation. Moreover, the angular power spectrum of the incident waves will be influenced by the surroundings of the different traffic environments, and it will differ depending on

the environment. For example, in rural environment there are few scattering objects in comparison to an urban or highway environment. These differences in the environments emphasize the need to evaluate the antennas under different conditions.

A possible solution to do this is to carry out measurement campaigns (i.e., drive tests). For example in [3]–[4] measurement campaigns have been carried out for the analysis of the antenna placement, while in [5–7] the propagation channel has been evaluated. Even though measurement campaigns are good alternatives, they are expensive and time consuming and not always possible in the early stages of product development. Therefore, it is desirable to find alternative methods (e.g., methods based on simulations) for repeatable and cost efficient evaluations of antennas under realistic conditions. There are a few alternative methods that have been published in the literature for the evaluation of the antenna performance: e.g., [8] has proposed a method that allows the optimization of antenna configurations using an antenna synthesis approach as well as ray tracing simulations, and [9] has modeled the propagation channel using a ray tracing approach to evaluate the antenna performance of three simulated single antennas placed at different positions. Another alternative method is the one presented in [10]. In this reference a method for evaluating the antenna performance for different antenna types, and antenna positions on the vehicle has been proposed. This method has used the antenna radiation patterns in combination with a multipath simulation tool. A key difference from these alternative methods is that here we estimate the propagation environment from a real multipath environment (i.e., measured) for evaluating the antenna performance.

In this paper we present a method for evaluating the V2V antenna performance under realistic conditions. This is done by using the antenna radiation pattern in combination with a multipath simulation tool [11] which in this paper is modified to simulate a realistic, measured-based multipath environment. In such environment, the angular power spectrum will differ according to the traffic environment. We characterize the environment with the relative average received power in four equal-sized sectors (front, left, back, and right). This results in three weight ( $W$ ) parameters

( $W_L$ ,  $W_B$ , and  $W_R$ ) which are acquired in a measurement campaign using a reference module which consists of four identical probe-fed patch antennas. The parameters are then used in a multipath simulation tool to simulate a realistic multipath environment. The antenna performance is then evaluated by studying the cumulative distribution function (CDF) for the voltages samples at the antenna port. Finally, the method is validated by using the radiation pattern of two V2V antennas mounted on the roof-top of a vehicle in combination with the simulation of the realistic multipath environment, and compared to validating measurement campaign. Comparison of simulated and measured received power CDFs indicates that the method is quite accurate.

The paper is organized as follows: In Section II the theory used to estimate the V2V propagation environment is presented. In Section III, the reference setup, the calibration of the system as well as the measurement campaign are described, and how the parameters that describe the V2V propagation environment are estimated. In Section IV, the proposed antenna evaluation method is described and the validation of the method together with the results are presented in Section V. Finally, conclusions are given in Section VI.

## II. THEORY

The average received power at the port of an antenna with radiation pattern  $\mathbf{G}(\theta, \varphi)$  due to an incident random complex electrical field  $\mathbf{E}(\theta, \varphi)$  is

$$\overline{P}_a = \mathbb{E} \left[ \left| \mathbf{G}(\theta, \varphi) \cdot \mathbf{E}(\theta, \varphi) \right|^2 \right], \quad (1)$$

where  $\mathbb{E}$  is the expectation operator,  $\theta$  is the polar angle, and  $\varphi$  is azimuth angle of the incident field.

The above equation is quite general. We will in the following make a number of simplifying assumptions to get tractable equations that are sufficiently accurate for our purposes. In summary, our assumptions on the propagation environment are

1) *The incident field consist of a number of vertically polarized, plane waves with statistically independent zero-mean complex Gaussian amplitudes*

2) *The waves arrive in the horizontal plane from statistically independent and uniformly distributed angle of arrivals*

3) *The angular power spectrum is constant in each of the four equal-sized sectors around the vehicle (front, left, back, right), see Fig. 1*

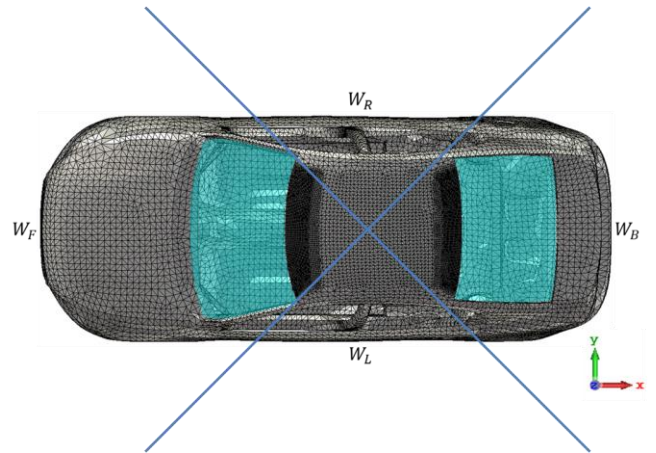


Figure 1. Top view of the vehicle where the azimuth plane is divided in four equal-sized sectors. The weights of each sector are represented by  $W_F$ ,  $W_L$ ,  $W_B$ ,  $W_R$ , (i.e., front, left, back, and right). The front of the vehicle is oriented towards the  $180^\circ$  direction (negative x-axis).

These three assumptions are described in detail below: In a V2V setting, it is reasonable to assume that propagation is confined to the horizontal plane, i.e., that  $\mathbf{E}(\theta, \varphi) = 0$  when  $\theta \neq \pi/2$ . If we furthermore assume that the electrical field is vertically polarized, we have that

$$\mathbf{G}(\theta, \varphi) \cdot \mathbf{E}(\theta, \varphi) = G(\varphi)E(\varphi) \quad (2)$$

where we have denoted the  $z$ -components of  $\mathbf{G}(\pi/2, \varphi)$  and  $\mathbf{E}(\pi/2, \varphi)$  by  $G(\varphi)$  and  $E(\varphi)$ , respectively.

For simplicity, we assume that the incident field consists of  $M$  plane waves,

$$E(\varphi) = \sum_{m=1}^M E_m(\varphi_m), \quad (3)$$

where  $\{E_1(\varphi_1), E_2(\varphi_2), \dots, E_M(\varphi_M)\}$  are modeled as statistically independent, zero-mean complex Gaussian random variables and where  $\{\varphi_1, \varphi_2, \dots, \varphi_M\}$  are modeled as statistically independent random variables uniformly distributed in  $[0, 2\pi)$ . The power density of the incident plane waves is normalized to one

$$\frac{1}{\eta} \left| \sum_{m=1}^M E_m(\varphi_m) \right|^2 = 1, \quad (4)$$

The variance (power) of the incident plane waves will typically depend on the angle of arrival. We express this as

$$E_m(\varphi_m) = E_m^{(i)} W(\varphi_m), \quad m = 1, 2, \dots, M \quad (5)$$

where  $W(\varphi)$  is a positive, real-valued deterministic function that is periodic with period  $2\pi$  and  $\{E_1^{(i)}, E_2^{(i)}, \dots, E_M^{(i)}\}$  are modeled as independent and identically distributed zero-mean complex Gaussian random variables with variance  $\mathbb{E} \left[ \left| E_m^{(i)} \right|^2 \right] = \sigma^2 / M$ .

As shown in the appendix, we can express the average received power at the antenna port as

$$\overline{P}_a = \mathbb{E} \left[ \left| \sum_{m=1}^M E_m^{(i)} W(\varphi_m) G(\varphi_m) \right|^2 \right] \quad (6)$$

$$= \sigma^2 \int_0^{2\pi} |W(v)G(v)|^2 \frac{1}{2\pi} dv. \quad (7)$$

As a final simplification, if we assume that  $W(\varphi)$  is piecewise constant in the forward, left, back, and right sectors, i.e.,

$$W(\varphi) = \begin{cases} W_F, & 3\pi/4 \leq \varphi < 5\pi/4 \\ W_L, & 5\pi/4 \leq \varphi < 7\pi/4 \\ W_B, & -\pi/4 \leq \varphi < \pi/4 \\ W_R, & \pi/4 \leq \varphi < 3\pi/4 \end{cases} \quad (8)$$

we can write

$$\overline{P}_a = \sigma^2 \left( W_F^2 |G_F|^2 + W_L^2 |G_L|^2 + W_B^2 |G_B|^2 + W_R^2 |G_R|^2 \right), \quad (9)$$

where

$$|G_F|^2 = \frac{1}{2\pi} \int_{3\pi/4}^{5\pi/4} |G(v)|^2 dv \quad (10a)$$

$$|G_L|^2 = \frac{1}{2\pi} \int_{5\pi/4}^{7\pi/4} |G(v)|^2 dv \quad (10b)$$

$$|G_B|^2 = \frac{1}{2\pi} \int_{-\pi/4}^{\pi/4} |G(v)|^2 dv \quad (10c)$$

$$|G_R|^2 = \frac{1}{2\pi} \int_{\pi/4}^{3\pi/4} |G(v)|^2 dv \quad (10d)$$

Hence,  $|G_x|^2$  is proportional to the average power gain in the sector  $X \in \{F, L, B, R\}$ .

We note that if  $G(\varphi) = W(\varphi) = 1$  for all  $\varphi$ , then the average received power at the antenna port is  $\overline{P}_a = \sigma^2$ , as expected.

### III. CALIBRATION AND MEASUREMENT CAMPAIGN

In order to estimate the parameters that describe the propagation environment based in our assumptions a reference system was designed, calibrated and used in a measurement campaign to acquire power samples in real vehicular propagation environments.

#### A. Reference Setup

Fig.2 and Fig.3 show the reference module which is mounted on a vehicle's roof. The module consists in four identical probe-fed patch antennas oriented outwards and placed far from each other. The distance between the antenna mounted on the front and the antenna mounted on the back is 4.30 m and the distance between the antennas mounted on the sides of the vehicle is 1.73 m. The patch antennas are

resonating at 5.9 GHz and their dimensions are 11 mm x 15 mm with respect to the vertical and horizontal plane, and a ground plane size of 100 x 160 mm. The substrate is FR4 with permittivity of 4.3, loss tangent of 0.025, and thickness of 1.6 mm.

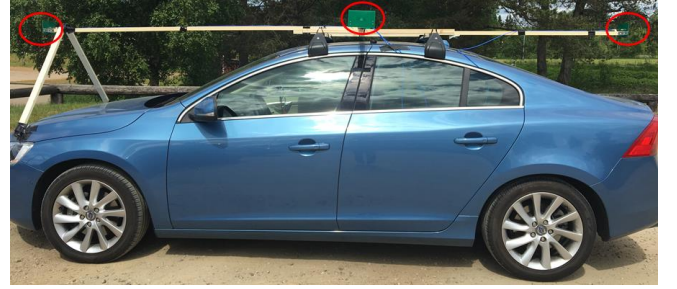


Figure 2. Side view of the vehicle using the reference module. The red circles show the placement of the outward facing patch antennas.

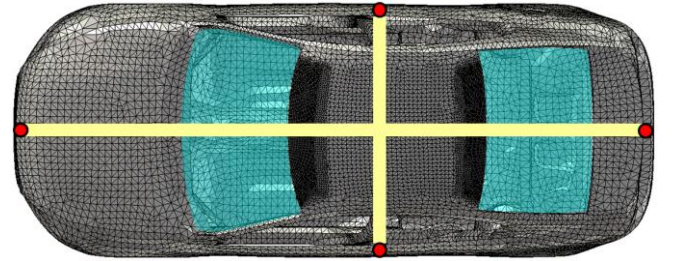


Figure 3. Top view of the vehicle using a reference module. The red circles represent the placement of the patch antennas which are facing outwards.

This reference module was first calibrated, as described in detail below, and then used in a measurement campaign. During measurements, two vehicles were used, a Volvo V70 on the transmitter side and a Volvo S60 on the receiver side. On the transmitter side a 5.9 GHz quarter-wave monopole antenna centrically mounted on a circular ground plane with radius of 50 mm was used. This antenna was mounted on the middle of the vehicle's roof-top. At the receiver side the reference module was used and mounted as shown in Fig. 2 and Fig. 3.

On the transmitter side a signal generator was used with output power set to 24 dBm. This was connected to the monopole antenna via an RF cable. On the receiver side the four antennas were connected to 4-port switch via RF cables which in turn were connected to a spectrum analyzer. The measurement setup collected four power samples per second during the measurements (i.e. one power sample per second per antenna).

#### B. Calibration of the System

The reference module antenna gain was obtained from measurements performed on a large open area (i.e., 70 x 100 m football field). For the measurements, the receiving vehicle was standing still and the transmitting vehicle was moving towards the receiving vehicle. Thus the incident waves were arriving to the front direction of the receiving vehicle. Then the average received power of each antenna

element was compared to obtain the sector gains in the horizontal plane. Finally, the gain is normalized to 0 dBi in its maximum direction, see Fig. 4. The same procedure could be applied to the other antenna elements. However, as mentioned before the antennas are identical, and therefore we assume that the gain of each antenna element is identical and constant in their four 90° sectors. Thus, the gain for the other antenna elements looks the same, but in a global coordinate system it will be rotated by 90°, 180°, and 270° clockwise for the right, back and left antenna. In this case, this is a reasonable method to obtain  $G$ , assuming that the antennas were not affected by the vehicle's body since they were mounted on the edge of the reference module, as can be seen in Fig. 2 and Fig. 3.

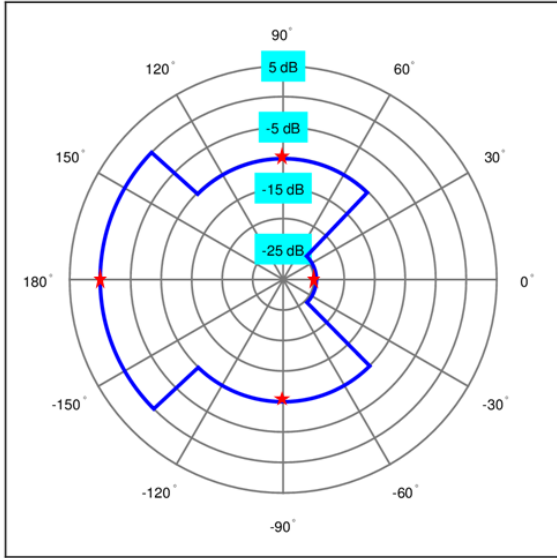


Figure 4. Gain of the reference antenna that is mounted in the front (180° direction, i.e., the negative x-axis). The red points represent a normalized measured average values per sector.

### C. Measurement Campaign

As mentioned before four power samples per second were collected during the measurements. This means one power sample per second per antenna. The data taken in this manner gives us the statistics that we need to estimate the change in the signal amplitude due to multipath components. This data is then used to calculate the parameters that describe the propagation environment. It should be pointed out that during measurements the vehicles were moving in a convoy and the transmitting vehicle was always in front of the receiving vehicle. This scenario was chosen because it is relevant for ITS applications.

The measurements were performed in three different road traffic environments, i.e., rural, urban, and highway. The *rural* measurements were performed outside the city of Borås in open surroundings. The speed during test on the rural road was between 50 - 70 km/h. At this road, there were very few reflecting and scattering objects affecting the propagation.

Measurements in the *urban* environment were performed in a densely populated area in the city of Borås. The streets

were narrow and there were many buildings and objects affecting the propagation environment. The average speed was approximately 20 km/h. The measurements in the *highway* environment were performed on a four lane highway, two lanes in each direction separated by a steel crash barrier. The speed was between 90 - 100 km/h during this test.

During all the measurements both vehicles were driving in the same direction and the distance of separation between the vehicles was varied between 40 to 80 m, 10 to 50 m, and 50 to 100 m in the rural, urban, and highway environment respectively.

### D. Parameter Calculations

In (9), we have derived the average received power for any antenna according to our assumptions on the propagation environment. This expression is now used to specify the average received power for the four antennas used in our reference module during the measurement campaign in a certain road traffic environment as

$$\bar{P}_a^F = \sigma^2 \left( W_F^2 |G_F^F|^2 + W_L^2 |G_L^F|^2 + W_B^2 |G_B^F|^2 + W_R^2 |G_R^F|^2 \right), \quad (11)$$

$$\bar{P}_a^L = \sigma^2 \left( W_F^2 |G_R^L|^2 + W_L^2 |G_F^L|^2 + W_B^2 |G_L^L|^2 + W_R^2 |G_B^L|^2 \right), \quad (12)$$

$$\bar{P}_a^B = \sigma^2 \left( W_F^2 |G_B^B|^2 + W_L^2 |G_R^B|^2 + W_B^2 |G_F^B|^2 + W_R^2 |G_L^B|^2 \right), \quad (13)$$

$$\bar{P}_a^R = \sigma^2 \left( W_F^2 |G_L^R|^2 + W_L^2 |G_B^R|^2 + W_B^2 |G_R^R|^2 + W_R^2 |G_F^R|^2 \right), \quad (14)$$

where  $\bar{P}_a^X$  denotes the average received power for the antenna in sector  $X \in \{F, L, B, R\}$  and  $G_Y^X$  denotes the gain of the X-sector antenna element in the direction of sector  $Y \in \{F, L, B, R\}$ .

These equations together with the average received power obtained from measurements and the gains obtained from the calibration in Sec. III.B are then used to calculate the parameters that describe the propagation environment in the following way

$$\begin{bmatrix} W_F^2 \sigma^2 \\ W_L^2 \sigma^2 \\ W_B^2 \sigma^2 \\ W_R^2 \sigma^2 \end{bmatrix} = \begin{bmatrix} |G_F^F|^2 & |G_L^F|^2 & |G_B^F|^2 & |G_R^F|^2 \\ |G_R^L|^2 & |G_F^L|^2 & |G_L^L|^2 & |G_B^L|^2 \\ |G_B^B|^2 & |G_R^B|^2 & |G_F^B|^2 & |G_L^B|^2 \\ |G_L^R|^2 & |G_B^R|^2 & |G_R^R|^2 & |G_F^R|^2 \end{bmatrix}^{-1} \cdot \begin{bmatrix} P_a^F \\ P_a^L \\ P_a^B \\ P_a^R \end{bmatrix} \quad (15)$$

Thus, the products of  $W_F$ ,  $W_L$ ,  $W_B$ , and  $W_R$ , with  $\sigma$  are calculated by (15), where  $G_Y^X$  is obtained from the calibration procedure described in Sec. III.B and  $P_a^X$  is

obtained from measurements described in Sec. III.C. These values are presented in Table I, where the weight in the forward direction  $W_F$  is normalized to 0 dB. It should be pointed out that the parameters were calculated individually for each traffic environment.

TABLE I. Parameters of the propagation model in each sector

	$W_F$ [dB]	$W_L$ [dB]	$W_B$ [dB]	$W_R$ [dB]
Rural	0	-4.3	-8.5	-4.0
Urban	0	-3.4	-9.2	-1.7
Highway	0	-5.2	-9.8	-4.6

#### IV. ANTENNA EVALUATION METHOD

The method for evaluating the V2V antenna performance under realistic conditions is done by using the radiation pattern of the antenna under test in combination with a simulation of a realistic multipath environment based on our assumptions on the propagation environment.

The antenna radiation pattern can be obtained by using any simulation software or measurements, and the simulation of the realistic multipath environment is done by using a multipath simulation tool [11] including the parameters calculated in (15), see Table I.

The multipath simulation tool [11] generates a multipath environment by a number of incident waves  $M$  defined by their AoA and polarization. These incident waves are then multiplied by the parameters estimated in Table I for each traffic environment. To simulate a changing environment as it is in reality, a large number of realizations must be generated when computing the received power. In each realization, a number of incident plane waves are combined with the antenna gain to produce a voltage sample at the antenna port. The corresponding power samples are collected and summarized in terms of a CDF. The CDFs from different antennas are then used to compare performance of the antennas.

#### V. VALIDATION OF THE METHOD

In order to validate our method two probe-fed patch antennas were used. The resonant frequency of the antennas was 5.9 GHz and they had a length of 11 mm, width of 15 mm and a ground plane size of 20 x 24 mm. The substrate was FR4 with permittivity of 4.3, loss tangent of 0.025, and thickness of 1.6 mm.

The antennas were placed on the middle of the roof-top of a vehicle and the distance of separation between them was 13 cm, as illustrated in Fig. 5. Antenna A was facing forward relative to the vehicle and antenna B was facing backward. This configuration was chosen to present a setup where both antennas were affected by the structure of the vehicle.

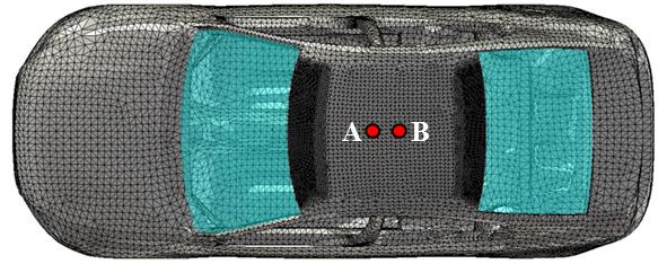


Figure 5. Top view of the vehicle using two validation antennas, antenna A and antenna B.

In Fig. 6 a block diagram of the validation procedure of the antenna evaluation method is shown. It consists of the comparison between a measurement campaign and simulations in three different road traffic environments.

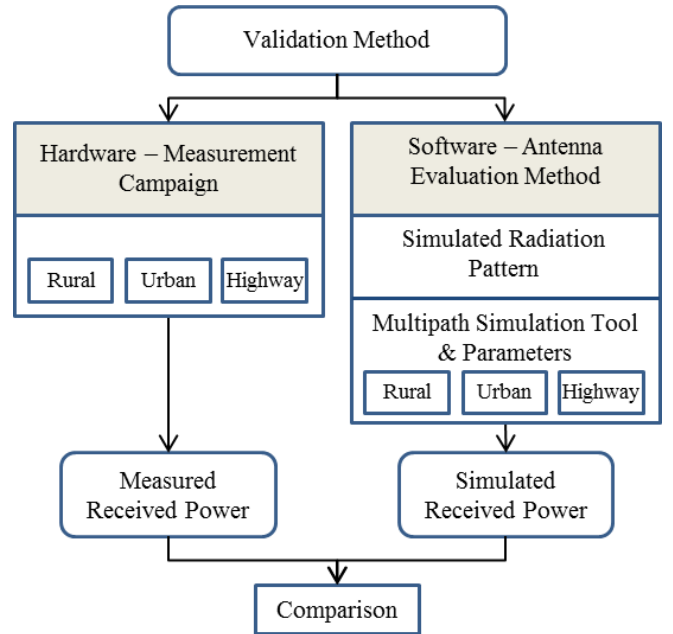


Figure 6. Block diagram of the validation of the method.

From measurements, we obtained the average received power. The collection of the data was done in a similar way as explained in Sec. III.C, where two vehicles were used, one on the transmitter side with a monopole antenna mounted on the roof-top of the vehicle and the other vehicle on the receiver side carrying the two patch antennas, see Fig. 5. The test roads were the same as the ones explained in Sec. III.C.

The simulations were performed according the antenna evaluation method explained in Sec. IV. The antenna radiation pattern was obtained using CST Microwave Studio [12] simulation software. The multipath environment was simulated with  $N = 10^5$  realizations and the number of vertically polarized incident waves was  $M = 30$  for all environments. It should be mentioned that the number of realizations  $N$  should be large enough to determine the CDFs accurately specially at lower levels, and the number of

incident waves  $M$  should be chosen to assure that at least 5 incident waves arrive to each sector.

The comparison between field measurements and simulations are done in terms of CDFs. For each data set the mean value was taken and then the difference between the CDFs curves was calculated.

Fig. 7-9 show the simulated and measured CDF curves of the received power for rural, urban and highway environment where the simulated average received power has been normalized to one. The figures show a good agreement between simulations and measurements. A closer comparison is done by taking the mean of each data set and calculating the difference between antenna A and antenna B. These results are shown in Tables II-IV. As it can be seen simulations and measurements agree well for the three environments.

### A. Performance of the Antennas

From the figures, we can determine which antenna performed better. As expected the forward facing antenna A performed better than the backward facing antenna B. This was because the transmitting antenna was always in front of the receiving vehicle during all the measurements.

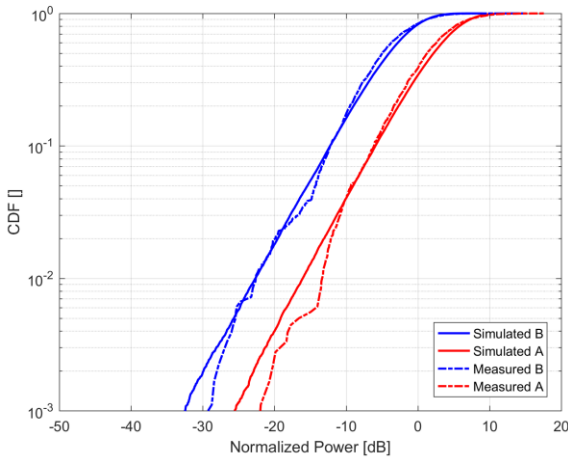


Figure 7. Simulated and measured CDF curves of the received power for the rural environment.

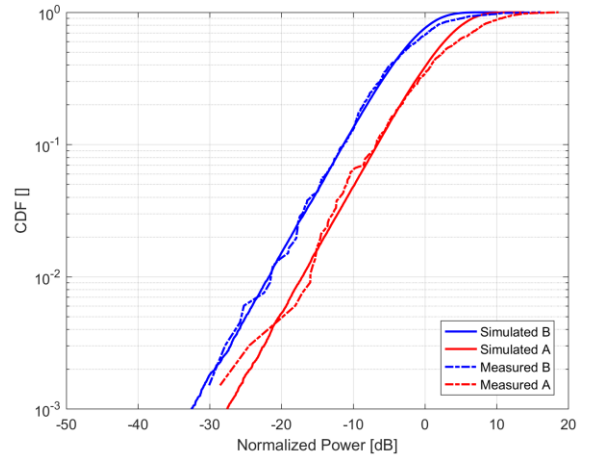


Figure 8. Simulated and measured CDF curves of the received power for the urban environment.

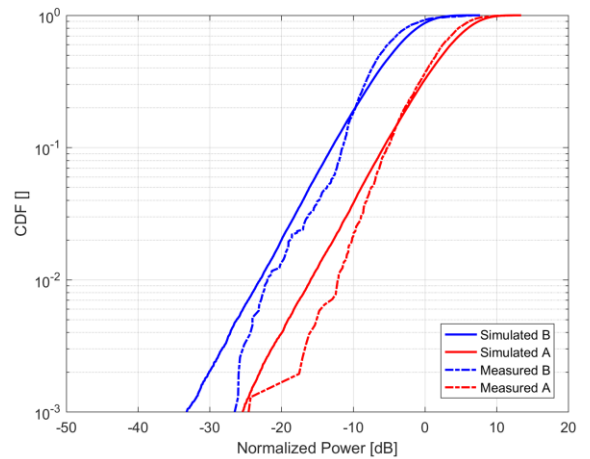


Figure 9. Simulated and measured CDF curves of the received power for the highway environment.

TABLE II. Difference in mean value of the measured and simulated received power in [dB] for the rural environment

	Measured	Simulated	$\Delta$ (Measured - Simulated)
A - B	6.1	5.9	0.2

TABLE III. Difference in mean value of the measured and simulated received power in [dB] for the urban environment

	Measured	Simulated	$\Delta$ (Measured - Simulated)
A - B	4.9	4.4	0.5

TABLE IV. Difference in mean value of the measured and simulated received power in [dB] for the highway environment

	Measured	Simulated	$\Delta$ (Measured - Simulated)
A - B	6.7	6.7	0

## VI. CONCLUSIONS

We have presented a method to evaluate vehicle mounted antennas in multipath environments. The method has been evaluated in three different road traffic environments and the

results of the comparison between field measurements and simulations show the validity of the method. The method is proposed as an alternative to field measurements. The method is fast, accurate, and can be used in the early stages of product development.

#### ACKNOWLEDGMENT

This work has been partly supported by the Swedish Governmental Agency for Innovation Systems (VINNOVA) within the VINN Excellence Center Chase.

#### APPENDIX

We denote the pdf for  $E_m^{(i)}$  by  $p_{E_m^{(i)}}(u_m)$  and the pdf for  $\varphi_m$  by  $p_{\varphi_m}(v_m)$ . Since the random variables are independent, the joint pdf of  $\{E_1^{(i)}, E_2^{(i)}, \dots, E_M^{(i)}, \varphi_1, \varphi_2, \dots, \varphi_M\}$  can be written as

$$p_{E,\varphi}(\mathbf{u}, \mathbf{v}) = p_E(\mathbf{u}) p_\varphi(\mathbf{v}), \quad (16)$$

where  $\mathbf{u} = [u_1 \ u_2 \ \dots \ u_M]$ ,  $\mathbf{v} = [v_1 \ v_2 \ \dots \ v_M]$ , and

$$p_E(\mathbf{u}) = \prod_{m=1}^M p_{E_m^{(i)}}(u_m), \quad (17)$$

$$p_\varphi(\mathbf{v}) = \prod_{m=1}^M p_{\varphi_m}(v_m). \quad (18)$$

From (6), we have that

$$\bar{P}_a = \mathbb{E} \left[ \left| \sum_{m=1}^M E_m^{(i)} W(\varphi_m) G(\varphi_m) \right|^2 \right] \quad (19)$$

$$= \int_{\mathbf{v}} \int_{\mathbf{u}} \left| \sum_{m=1}^M u_m W(v_m) G(v_m) \right|^2 p_E(\mathbf{u}) p_\varphi(\mathbf{v}) d\mathbf{u} d\mathbf{v} \quad (20)$$

$$= \int_{\mathbf{v}} \left[ \int_{\mathbf{u}} \left| \sum_{m=1}^M u_m W(v_m) G(v_m) \right|^2 p_E(\mathbf{u}) d\mathbf{u} \right] p_\varphi(\mathbf{v}) d\mathbf{v} \quad (21)$$

The expression inside the brackets is simply the variance of the random variable  $\sum_{m=1}^M E_m^{(i)} W(v_m) G(v_m)$ , which in turn is a sum of  $M$  independent random variables, where the  $m$ th random variable has variance  $(\sigma^2/M) |W(v_m) G(v_m)|^2$ .

Hence,

$$\begin{aligned} & \int_{\mathbf{u}} \left| \sum_{m=1}^M u_m W(v_m) G(v_m) \right|^2 p_E(\mathbf{u}) d\mathbf{u} \\ &= \frac{\sigma^2}{M} \sum_{m=1}^M |W(v_m) G(v_m)|^2, \end{aligned} \quad (22)$$

and

$$\bar{P}_a = \frac{\sigma^2}{M} \sum_{m=1}^M \int_{\mathbf{v}} |W(v_m) G(v_m)|^2 p_\varphi(\mathbf{v}) d\mathbf{v} \quad (23)$$

The multidimensional integral simplifies to

$$I_m = \int_{\mathbf{v}} |W(v_m) G(v_m)|^2 p_\varphi(\mathbf{v}) d\mathbf{v} \quad (24)$$

$$= \int_{v_m} |W(v_m) G(v_m)|^2 p_{\varphi_m}(v_m) dv_m \quad (25)$$

$$= \int_{v_m} |W(v_m) G(v_m)|^2 \frac{1}{2\pi} dv_m \quad (26)$$

where (25) follows since  $|W(v_m) G(v_m)|^2$  is a constant when integrating over  $v_1, v_2, \dots, v_{m-1}, v_{m+1}, \dots, v_M$ . The integrand can be viewed as a periodic function with period  $2\pi$ , and we can choose the integration interval to any interval of length  $2\pi$ , e.g.,

$$\begin{aligned} I_m &= \int_0^{2\pi} |W(v_m) G(v_m)|^2 \frac{1}{2\pi} dv_m \\ &= \frac{W_F^2}{2\pi} \int_{3\pi/4}^{5\pi/4} |G(v_m)|^2 dv_m \\ &\quad + \frac{W_L^2}{2\pi} \int_{5\pi/4}^{7\pi/4} |G(v_m)|^2 dv_m \\ &\quad + \frac{W_B^2}{2\pi} \int_{-\pi/4}^{\pi/4} |G(v_m)|^2 dv_m \\ &\quad + \frac{W_R^2}{2\pi} \int_{\pi/4}^{3\pi/4} |G(v_m)|^2 dv_m \end{aligned} \quad (27)$$

$$I_m = W_F^2 |G_F|^2 + W_L^2 |G_L|^2 + W_B^2 |G_B|^2 + W_R^2 |G_R|^2 \quad (28)$$

where we have used the fact that the weight function  $W(\varphi)$  is piece-wise constant, as shown in (8). Using (23) and (28), we can write

$$\begin{aligned} \bar{P}_a &= \frac{\sigma^2}{M} \sum_{m=1}^M I_m \\ &= \sigma^2 \left( W_F^2 |G_F|^2 + W_L^2 |G_L|^2 + W_B^2 |G_B|^2 + W_R^2 |G_R|^2 \right), \end{aligned} \quad (29)$$

which proves (9) and (10).

#### REFERENCES

- [1] E. G. Ström, "On Medium Access and Physical Layer Standards for Cooperative Intelligent Transport Systems in Europe," *Proceedings of the IEEE*, vol. 99, no. 7, pp. 1183-1188, July 2011.
- [2] J. B. Kenney, "Dedicated Short-Range Communications (DSRC) Standards in the United States," *Proceedings of the IEEE*, vol. 99, no. 7, pp. 1162-1182, July 2011.

- [3] T. Abbas, J. Karedal, and F. Tufvesson, "Measurement-Based Analysis: The Effect of Complementary Antennas and Diversity on Vehicle-to-Vehicle Communication," *IEEE Antennas and Wireless Propagation Letters*, vol. 12, pp. 309-312, Mar. 2013.
- [4] K. Karlsson, J. Carlsson, M. Olbäck, T. Vukusic, R. Whiton, S. Wickström, *et al.*, "Utilizing Two-Ray Interference in Vehicle-to-Vehicle Communications," *Antennas and Propagation (EuCAP) Proceedings of the 8th European Conference*, The Hague, The Netherlands, April 2014.
- [5] T. Abbas, L. Bernadó, A. Thiel, C. Mecklenbräuker, and F. Tufvesson, "Radio Channel Properties for Vehicular Communication: Merging Lanes Versus Urban Intersections," *IEEE Vehicular Technology Magazine*, pp. 27-34, Nov. 2013.
- [6] K. Karlsson, C. Berghem, and E. Hedin, "Field Measurements of IEEE 802.11p Communication in NLOS Environments for a Platooning Application," in *IEEE Vehicular Technology Conference. VTC 2012-Fall*, Quebec, Canada, Sept. 2012.
- [7] J. Karedal, F. Tufvesson, T. Abbas, O. Klemp, A. Paier, L. Bernadó, *et al.*, "Radio Channel Measurements at Street Intersections for Vehicle-to-Vehicle Safety Applications," in *IEEE Vehicular Technology Conference. VTC 2010-Spring Taipei*, Taiwan, May 2010.
- [8] L. Reichardt, J. Pontes, W. Wiesbeck, and T. Zwick, "Virtual Drives in Vehicular Communication Optimization of MIMO Antenna Systems," *IEEE Vehicular Technology Magazine*, pp. 54-62, June 2011.
- [9] D. Kornek, M. Schack, E. Slotke, O. Klemp, I. Rolfes, and T. Kürner, "Effects of Antenna Characteristics and Placements on a Vehicle-to-Vehicle Channel Scenario," in *IEEE International Conference on Communications Workshops (ICC)*, Capetown, South Africa, May 2010.
- [10] E. Condo Neira, U. Carlberg, J. Carlsson, K. Karlsson, and E. G. Ström, "Evaluation of V2X Antenna Performance Using a Multipath Simulation Tool," *Antennas and Propagation (EuCAP) Proceedings of the 8th European Conference*, The Hague, The Netherlands, April 2014.
- [11] U. Carlberg, J. Carlsson, A. Hussain, and P. S. Kildal, "Ray Based Multipath Simulation Tool for Studying Convergence and Estimating Ergodic Capacity and Diversity Gain for Antennas with Given Far-Field Functions," in *20th Internat. Conf. on Applied Electromagnetics and Communications (ICECom)*, Dubrovnik, Croatia, Sept. 2010.
- [12] CST Microwave Studio. Available: <https://www.cst.com/>